การสังเคราะห์บีดพอลิเมอร์หลายชั้นที่มีสมบัติการกระเจิงรังสีอัลตราไวโอเลต

นางสาวรัศมี แสงศิริมงคลยิ่ง

วิทยานิพนธ์นี้เป็นส่วนหนึ่งของการศึกษาตามหลักสูตรปริญญาวิทยาศาสตรดุษฎีบัณฑิต
สาขาวิชาเคมีเทคนิค ภาควิชาเคมีเทคนิค
คณะวิทยาศาสตร์ จุฬาลงกรณ์มหาวิทยาลัย
ปีการศึกษา 2544

ISBN 974-03-1139-3

SYNTHESIS OF MULTI-LAYERED POLYMER BEADS WITH UV SCATTERING PROPERTY

Miss Ratsamee Sangsirimongkolying

A Dissertation Submitted in Partial Fulfillment of the Requirements
for the Degree of Doctor of Philosophy in Chemical Technology
Department of Chemical Technology
Faculty of Science
Chulalongkorn University
Academic Year 2001

ISBN 974-03-1139-3

Thesis Title	SYNTHESIS OF MULTI-LAYERED POLYMER BEADS WITH UV SCATTERING PROPERTY
By	Miss Ratsamee Sangsirimongkolying
Field of study	Chemical Technology
Thesis Advisor	Professor Somsak Damronglerd, Dr. Ing.
Thesis Co-advisor	Professor Suda Kiatkamjornwong, Ph.D.
Thesis Co-advisor	Professor Shinzo Omi, Ph.D.

Accepted by the Faculty of Science, Chulalongkorn University in Partial Fulfillment of the Requirements for the Doctor's Degree

…… Deputy Dean for Administrative Affairs
Acting Dean, Faculty of Science

(Associate Professor Pipat Karntiang, Ph.D.)

THESIS COMMITTEE

…… Chairman

(Associate Professor Pornpote Piumsomboon, Ph.D.)

…….. Thesis Advisor

(Professor Somsak Damronglerd, Dr. Ing.)

…….. Thesis Co-advisor

(Professor Suda Kiatkamjornwong, Ph.D.)

…….. Thesis Co-advisor

(Professor Shinzo Omi, Ph.D.)

…….. Member

(Assistant Professor Somkiat Ngamprasertsith, Dr.de l'INPT)

…….. Member

(Dr. Sangobtip Pongstabodee, Ph.D.)

…….. Member

(Dr. Nopporn Pramojaney, Ph.D.)

##4173818323 : MAJOR CHEMICAL TECHNOLOGY

KEY WORD : COMPOSITE POLYMER / PDMAEMA / PMMA / PST / SEEDED EMULSION POLYMERIZATION

RATSAMEE SANGSIRIMONGKOLYING: SYNTHESIS OF MULTI-LAYERED POLYMER BEADS WITH UV SCATTERING PROPERTY. THESIS ADVISOR: PROF. SOMSAK DAMRONGLERD, Dr. Ing. THESIS CO-ADVISORS: PROF. SUDA KIATKAMJORNWONG, Ph.D. AND PROF. SHINZO OMI, Ph.D., 100 pp. ISBN 974-03-1139-3

Syntheses of three-novel types of multi-layered polymer beads, poly[(dimethyl aminoethyl methacrylate)-*co*-ST]/poly(methyl methacrylate)/polystyrene [P(DMAEMA-*co*-ST)/PMMA/PST] composite particles, with UV scattering property have been prepared successfully by the seeded emulsion polymerization using the following three steps. First, emulsion polymerization of P(DMAEMA-*co*-ST) seed latex was carried out using cetyltrimethyl ammonium chloride (CTAC) as a cationic stabilizer. The particle size of P(DMAEMA-*co*-ST) particles could be controlled by CTAC and 2,2'-azobis(2-amidinopropane)•2HCl (V-50) concentrations. Second, methyl methacrylate (MMA) monomer was added into P(DMAEMA-*co*-ST) seed latex by dropwise method. It is found that the initiator types, V-50 or potassium persulfate (KPS), were the key factor for the morphology control of P(DMAEMA-*co*-ST)/PMMA composite particles. P(DMAEMA-*co*-ST)/PMMA composite particles were halfmoon-like morphology surrounded by the P(DMAEMA-*co*-ST)-rich phase when V-50 was used as an initiator, while a small P(DMAEMA-*co*-ST)-rich phase distributed inside of the PMMA-rich phase and inverted core-shell composite particles were produced when KPS was employed. Finally, P(DMAEMA-*co*-ST)/PMMA/PST composite particles were thus synthesized by seeded polymerization, using the above latex as the seed polymer and ST as the final-stage monomer. It was found that P(DMAEMA-*co*-ST)/PMMA seed particles were always surrounded by the PST-rich shell using V-50 as the initiator, while PS-rich phase partially engulfed by the P(DMAEMA-*co*-ST)-rich phase as a core covered by the PMMA-rich shell was obtained when the hydrophilic P(DMAEMA-*co*-ST)/PMMA composite particles having the lower molecular weight were used. The crosslinked P(DMAEMA-*co*-ST) seed particles of the first step did not affect the morphology of composite polymers. The refractive index depended on the morphology and particle size of composite polymers. The optimum morphology of composite polymers with a UV scattering property constituted a PMMA core containing small P(DMAEMA-*co*-ST) domains surrounded by the PST-rich shell. The reflection of which was 7.51% (n= 1.755).

Department…Chemical Technology.. Student's signature……

Field of study...Chemical Technology. Advisor's signature……

Academic year……2001…… Co-advisor's signature……...

Co-advisor's signature……...

รัศมี แสงศิริมงคลยิ่ง : การสังเคราะห์บีดพอลิเมอร์หลายชั้นที่มีสมบัติการกระเจิงรังสีอัลตราไวโอเลต. (SYNTHESIS OF MULTI-LAYERED POLYMER BEADS WITH UV SCATTERING PROPERTY) อาจารย์ที่ปรึกษา : ศาสตราจารย์ ดร. สมศักดิ์ ดำรงค์เลิศ อาจารย์ที่ปรึกษาร่วม : ศาสตราจารย์ ดร. สุดา เกียรติกำจรวงศ์ และ Prof. Dr. Shinzo Omi, 100 หน้า. ISBN 974-03-1139-3

การสังเคราะห์บีดพอลิเมอร์หลายชั้นพอลิไดเมทิลอะมิโนเอทิลเมทาคริเลต-*โค*-สไตรีน/พอลิเมทาคริเลต/พอลิสไตรีน [P(DMAEMA-*co*-ST)/PMMA/PST] แบบใหม่ 3 ชนิด ที่มีสมบัติการกระเจิงแสงอัลตราไวโอเลต โดยปฏิกิริยาซีดเดตอิมัลชันพอลิเมอไรเซชัน ซึ่งประกอบด้วย 3 ขั้นตอน คือ การเตรียม P(DMAEMA-*co*-ST) ด้วยปฏิกิริยาอิมัลชันพอลิเมอไรเซชัน โดยใช้ซิทิลไทเมทิลแอมโมเนียมคลอไรด์ (CTAC) เป็นสารลดแรงตึงผิว ซึ่งพบว่าขนาดอนุภาค P(DMAEMA-co-ST) สามารถควบคุมได้ด้วยตัวแปรความเข้มข้นของ CTAC และ 2,2'-เอโซบีส(2-อะมิไดโนโพเพน)ไดไฮโดรคลอริกแอซิด (V-50) จากนั้นเติมมอนอเมอร์เมทิลเมทาคริเลตลงในซีด P(DMAEMA-*co*-ST) ด้วยวิธีการหยด ซึ่งพบว่าชนิดของสารริเริ่ม (V-50 และโพแทสเซียมเพอร์ซัลเฟต) เป็นตัวแปรสำคัญต่อโครงสร้างของอนุภาคเชิงซ้อน P(DMAEMA-*co*-ST)/PMMA คือเมื่อใช้ V-50 เป็นสารริเริ่ม อนุภาคเชิงซ้อน P(DMAEMA-*co*-ST)/PMMA มีลักษณะแบ่งครึ่งและถูกหุ้มด้วยเฟส P(DMAEMA-*co*-ST) ในขณะที่เฟส P(DMAEMA-*co*-ST) กระจายในเฟส PMMA ซึ่งเคลื่อนจากผิวเข้าสู่ภายในอนุภาค เมื่อใช้โพแทสเซียมเพอร์ซัลเฟตเป็นสารริเริ่ม และขั้นตอนสุดท้ายการเตรียมอนุภาคเชิงซ้อน P(DMAEMA-*co*-ST)/PMMA/PST ด้วยปฏิกิริยาซีดเดตอิมัลชันพอลิเมอไรเซชัน โดยใช้ซีดพอลิเมอร์ที่เตรียมได้จากขั้นตอนที่แล้วและใช้สไตรีนเป็นมอนอเมอร์ ซึ่งพบว่าอนุภาค P(DMAEMA-*co*-ST)/PMMA ถูกหุ้มด้วยชั้นพอลิสไตรีน เมื่อใช้อนุภาคเชิงซ้อน P(DMAEMA-*co*-ST)/PMMA ที่มีน้ำหนักโมเลกุลสูง ในขณะที่พอลิสไตรีนถูกหุ้มด้วย P(DMAEMA-*co*-ST) เป็นแกนภายใน ถูกหุ้มด้วยพอลิเมทิลเมทาคริเลตที่เคลื่อนที่ออกมาที่ผิวอนุภาค เมื่อใช้อนุภาคเชิงซ้อน P(DMAEMA-*co*-ST)/PMMA ที่มีน้ำหนักโมเลกุลต่ำกว่า การเติมสารเชื่อมขวางใน P(DMAEMA-*co*-ST) ไม่ส่งผลกระทบต่อโครงสร้างของพอลิเมอร์เชิงซ้อนและมีผลทำให้เกิดการรวมตัวกันเป็นก้อนในทุกขั้นตอน ค่าดรรชนีหักเหของพอลิเมอร์เชิงซ้อน P(DMAEMA-*co*-ST)/PMMA/PST ขึ้นอยู่กับโครงสร้างและขนาดอนุภาค โครงสร้างที่เหมาะสมของพอลิเมอร์เชิงซ้อนที่มีสมบัติการกระเจิงแสงอัลตราไวโอเลตประกอบด้วย แกนพอลิเมทราคริเลต ที่มี P(DMAEMA-*co*-ST) เม็ดเล็กกระจายและถูกหุ้มด้วยชั้นพอลิสไตรีน ซึ่งสามารถสะท้อนแสงกลับได้ร้อยละ 7.51 (ค่าดรรชนีหักเห = 1.755)

ภาควิชา...เคมีเทคนิค.....ลายมือชื่อนิสิต.....

สาขาวิชา...เคมีเทคนิค..... ลายมือชื่ออาจารย์ที่ปรึกษา.....

ปีการศึกษา...2544..... ลายมือชื่ออาจารย์ที่ปรึกษาร่วม.....

ลายมือชื่ออาจารย์ที่ปรึกษาร่วม.....

ACKNOWLEDGEMENTS

The author would like to acknowledge my heartfelt gratitude and appreciation to her advisors, Professor Dr. Somsak Damronglerd, Prof. Dr. Suda Kiatkamjornwong and Prof. Dr. Shinzo Omi for their kind supervision, invaluable guidance, constant encouragement review and correction of the dissertation content.

The author is also sincerely grateful to Prof. Dr. Guang-Hui Ma for her comment, suggestions, and help in Omi's laboratory in Japan. Also, particular thanks are conveyed to Mr. Hiroaki Ando (Central Research Laboratory, Konica Co., Japan) who kindly carried out the light scattering measurement.

The author also greatly appreciate the Royal Golden Jubilee (RGJ) project of the Thailand Research Fund (TRF) for providing a three-year scholarship to the author to carry out part of the research at Graduate School of Bio-Applications and Systems Engineering (BASE) of the Tokyo University of Agriculture and Technology. Research facilities at the Department of Chemical Technology, the Department of Imaging and Printing Technology at the initial stage of the experimental work are highly appreciated.

The author also many thanks to the members of the dissertation committee for their comment, suggestions, and time to read the dissertation.

Special thanks to Assistant Professor Kiranant Ratanathammapan at the Department of Physic for providing facility for preparing the refractive index equipment and Assistant Professor Dr. Sanong Angkasit at the Department of Chemistry for his help in preparing film samples by spin coating.

Thanks are due to the doctor students at BASE for their assistance in instrument operations: Du Yongzhong, Ni Henmei, Fuminori Ito, Naoshiro Yamazaki,

Anchali Supsakulchai, and to the master students: Junichiro Fujiwara, Chen Aiyi, Ann Chorujun, Masahiro Fujioka, Shigeo Eda, Miho Watanabe, Tetsuro Ichikawa; and the visiting researchers: Mr. Mu Rui from China; Mrs. Kusoomjin Srirattnai from Thailand, who worked together with me in Omi's laboratory. Many thanks go to my friends in Thailand whose names are not mentioned here for their assistance and encouragement during the period of this study.

Finally, and most of all, the author would like to express her deep gratitude to her family and Miss Nualhathai T.Chaisuwan for their love, inspiration, understanding and endless encouragement throughout this entire study.

Ratsamee Sangsirimongkolying

CONTENTS

PAGE

ABSTRACT (IN THAI)…… iv

ABSTRACT (IN ENGLISH)……. v

ACKNOWLEDGEMENT……. vi

CONTENTS…….. viii

LIST OF TABLES……. xiv

LIST OF FIGURES…… xv

ABBREVIATIONS…… xix

CHAPTER I: INTRODUCTION……... 1

1.1 Scientific Background and Rationale…….. 1

1.2 Objectives of Research Work……...……. 2

1.3 Scopes of Research Work……. 2

1.4 Contents of Research Work…….. 4

CHAPTER II: THEORY AND LITERATURE REVIEW...……. 6

2.1 Dispersion Polymerization…… 6

2.2 Suspension Polymerization……... 8

2.3 Emulsion Polymerization…….. 9

2.3.1 Role of Limited Aggregation in Particle Nucleation….. 12

2.4 Composite Latex Particle Morphology……. 13

2.4.1 Preparation of Composite Particle Structure……... 13

2.4.1.1 Seeded Emulsion Polymerization…… 13

2.4.1.2 Heterocoagulation…… 15

CONTENTS (continued)

PAGE

2.5 Important Polymerization Parameters in Controlling Particle Morphology…….. 17

2.5.1 Effect of Polymer/Water Interfacial Tension and Particle Surface Polarity…… 17

2.5.2 Effect of Surfactant…… 17

2.5.3 Effect of Mode of Monomer Addition…….. 17

2.5.4 Effect of Polymer Crosslinking Agents……. 18

2.6 Optical Properties…… 18

2.6.1 Refractive Index…….. 18

2.6.2 Total internal reflection……. 19

2.6.3 Light Transmission and Gloss…… 20

2.7 Literature Review……. 22

CHAPTER III: EXPERIMENTAL…… 33

3.1 Chemicals

3.1.1 Monomer……. 33

3.1.2 Initiator…… 33

3.1.3 Suspending Agent…… 33

3.1.4 Crosslinking Agent…….. 34

3.1.5 Solvents…… 34

3.1.6 Other Chemicals……... 34

3.2 Glassware…….. 35

CONTENTS (continued)

PAGE

3.3 Equipment……. 35

3.4 Polymerization Procedures…… 35

3.4.1 Preparation of PDMAEMA Core Particles…….. 36

3.4.1.1 Dispersion Polymerization…….. 36

3.4.1.2 Suspension Polymerization……. 36

3.4.1.3 Emulsion Polymerization…… 36

3.4.2 Preparation of PMMA Shell by Seeded Emulsion Polymerization…… 37

3.4.2.1 Swelling Method……. 37

3.4.2.2 Drop-by-Drop Method…… 37

3.4.3 Preparation of PST Outer Shell…….. 37

3.4.3.1 Heterocoagulation…….. 37

3.4.3.1.1 Preparation of Cationic PST emulsion…….. 37

3.4.3.1.2 Preparation of Anionic P(DMAEMA -*co*-ST)/PMMA Particles……. 38

3.4.3.1.3 Blend Emulsion by the Stepwise Heterocoagulation Method…….. 38

3.4.3.2 Seeded Emulsion Polymerization…… 38

3.5 Characterization…… 38

3.5.1 Conversion…… 38

3.5.2 Scanning Electron Microscopy…… 39

CONTENTS (continued)

PAGE

3.5.3 Light Scattering…… 40

3.5.4 Transmission Electron Microscopy…….. 40

3.5.5 Thermal Properties of Polymers…….. 40

3.5.6 Gel Permeation Chromatography…… 41

3.5.7 Zeta Potential…… 41

3.5.8 Refractive Index…… 42

CHAPTER IV: RESULTS AND DISSCUSSION…….. 43

4.1 Preparation of PDMAEMA Core Particles……..… 43

4.1.1 Dispersion Polymerization…… 43

4.1.1.1 Effect of Solvent Type…….. 43

4.1.1.2 Effect of Solvent Composition……44

4.1.2 Suspension Polymerization…… 46

4.1.2.1 Effect of the Crosslinking Agent…… 46

4.1.2.2 Effect of the Ethyl Acetate Concentration……. 49

4.1.2.3 Effect of Electrolyte Concentration…….. 52

4.1.2.4 Effect of Co-monomer Type.…… 55

4.1.2.5 Effect of Solvent Type.…… 55

4.1.2.6 Effect of Polymerization Temperature…….. 56

4.1.2.7 Effect of Stabilizer Type.…….. 58

4.1.2.8 Effect of ST Content in Monomer…… 59

4.1.3 Emulsion Polymerization…….. 60

4.1.3.1 Effect of CTAC Concentration……. 60

CONTENTS (continued)

PAGE

4.1.3.2 Effect of Initiator Type..... 63

4.1.3.3 Effect of Crosslinking Agent Type..... 64

4.1.3.4 Effect of V-50 Concentration..... 66

4.2 Preparation of PMMA Shells by Seeded Emulsion Polymerization..... 68

4.2.1 Swelling Method..... 68

4.2.2 Drop-by-Drop Method..... 70

4.2.2.1 Effect of the Initiator Type..... 70

4.2.2.2 Effect of Particle Size of P(DMAEMA-co-ST) Seed..... 73

4.2.2.3 Effect of Crosslinking Agent Type of P(DMAEMA -*co*-ST) Seed..... 75

4.3 Preparation of PST Outer Shells by Seeded Emulsion Polymerization..... 76

4.3.1 Heterocoagulation..... 76

4.3.1.1 Cationic PST Emulsion..... 76

4.3.1.2 Anionic P(DMAEMA-co-ST)/PMMA Particles... 77

4.3.1.3 Blend Emulsion by the Stepwise Heterocoagulation Method..... 78

4.3.1.3.1 Effect of SDS Concentration..... 78

4.3.2 Seeded Emulsion Polymerization of P(DMAEMA-co-ST) /PMMA/PST..... 80

CONTENTS (continued)

PAGE

4.3.2.1 Morphology of the P(DMAEMA-*co*-ST)/PMMA/PST Composite Particles……..81

4.4 Properties of Composite Polymers……. 85

4.4.1 Average Molecular Weight of Composite Polymers…….85

4.4.2 Refractive Index of Composite Polymers……..87

4.4.2.1 Latex Film Formation…… 87

4.4.2.2 Evaluation of Film Index…….87

CHAPTER V: CONCLUSIONS AND SUGGESTIONS…….. 90

5.1 Conclusions…….. 90

5.1.1 Preparation of PDMAEMA Core Particles…….90

5.1.2 Preparation of PMMA Shells and PST Shells…… 91

5.2 Suggestions for Future Work…….. 92

REFERENCES…….. 93

VITA……. 100

LIST OF TABLES

TABLE **PAGE**

4.1 Recipe of P(DMAEMA-*co*-ST) seed particles by dispersion polymerization…… 44

4.2 Recipe of PDMAEMA Seed Particles by Suspension Polymerization... 47

4.3 Glass transition temperature of the PDMAEMA copolymers……. 54

4.4 Recipe of P(DMAEMA-*co*-ST) Seed Particles by Emulsion Polymerization……. 61

4.5 Recipe of P(DMAEMA-co-ST)/PMMA particles by seeded emulsion polymerization…… 71

4.6 Recipes of heterocoagulation for the preparations of cationic small PST particles and anionic large P(DMAEMA-*co*-ST) particles……..… 79

4.7 Recipe of P(DMAEMA-co-ST)/PMMA/PS composite particles by seeded emulsion polymerization…… 81

4.8 Characterization of P(DMAEMA-*co*-ST)/PMMA composite polymers…… 86

4.9 Characterization of P(DMAEMA-*co*-ST)/PMMA/PST composite polymers…… 86

4.10 Refractive Indices of P(DMAEMA-*co*-ST)/PMMA/PST composite polymers…… 89

LIST OF FIGURES

FIGURE PAGE

2.1 Schematic homogeneous nucleation mechanism in dispersion polymerization……. 7

2.2 Schematic micellar nucleation mechanism (Harkin's theory) in emulsion polymerization……. 10

2.3 Schematic homogeneous nucleation mechanism in emulsion polymerization……. 11

2.4 Heterocoagulation: (a) surface coating by small latex particles; (b) network formation; (c) encapsulation; (d) engulfment…… 16

2.5 Total internal reflection. The angle of incidence ϕ_c, for which the angle of refraction is 90^o, is called the critical angle…… 20

3.1 M-line method setup: (1) He-Ne Laser source (632.8 nm), (2) polarizer rotator, (3) polarizer, (4) prism, (5) film on a fused-silica plate, (6) X-Y stage, (7) rotation state, (8) screen…… 42

4.1 SEM photographs of P(DMAEMA-*co*-ST) particles for various ratios of water to iso-butanol : (a) 30:70 (Run 19), (b) 40:60 (Run 18), (c) 50:50 (Run 6)……. 45

4.2 SEM micrograph of the crosslinked P(DMAEMA-*co*-ST) particles using AIBN dissolved in acetone (Run 110)…… 49

4.3 SEM micrographs of the uncrosslinked P(DMAEMA-*co*-MMA) particles for various concentrations of ethyl acetate: (a) 2.8 wt% (Run 115); (b) 5.8 wt% (Run 119); (c) 9.0 wt% (Run 117)…… 50

4.4 Dependence of the particle size of P(DMAEMA-co-MMA) on the concentration of ethyl acetate in the continuous phase……. 51

LIST OF FIGURES (continued)

FIGURE PAGE

4.5 SEM photographs of the uncrosslinked P(DMAEMA-*co*-MMA) particles for various concentrations of Na_2SO_4 electrolyte: (a) 10^{-3} M (Run 121); (b) 10^{-2} M (Run 120)…..…… 52

4.6 SEM photograph of the uncrosslinked P(DMAEMA-*co*-ST) particles using AIBN dissolved in ethyl acetate (Run 129)……. 54

4.7 SEM photograph of the uncrosslinked P(DMAEMA-*co*-ST) particles using AIBN dissolved in acetone (Run 133)…… 56

4.8 SEM photographs of the uncrosslinked P(DMAEMA-*co*-ST) particles prepared at various polymerization temperatures: (a) 333 K (Run 137); (b) 338 K (Run 136); (c) 348 K (Run 134)…… 57

4.9 SEM photograph of the uncrosslinked P(DMAEMA-*co*-ST) particles with 50% ST content in monomers (Run 145)…… 60

4.10 Histograms of the size distribution of the uncrosslinked P(DMAEMA-*co*-ST) particles using different concentrations of CTAC: (a) 0.65 wt% (Run 153); (b) 1.30 wt% (Run 154); (c) 2.50 wt% (Run 152)…… 62

4.11 Histograms of the size distribution of the crosslinked P(DMAEMA-*co*-ST) particles using different crosslinking agents: (a) DVB (Run 157); (b) EGDMA (Run 159)…… 65

4.12 Histogram of the size distribution of the uncrosslinked P(DMAEMA-*co*-ST) particles using 5.0 wt% of V-50 (Run 160)……. 67

4.13 TEM photograph of P(DMAEMA-*co*-ST)/PMMA composite particles (Run 202) prepared by swelling method…… 69

LIST OF FIGURES (continued)

FIGURE PAGE

4.14 TEM photographs of P(DMAEMA-*co*-ST)/PMMA composite particles using various initiator types; (a) Seed: Run 153 with V-50 (Run217), (b) Seed 154 with KPS (Run 218). [P(DMAEMA-*co*-ST) domain was stained with RuO_4]…….. 72

4.15 TEM photograph of P(DMAEMA-*co*-ST)/PMMA composite particles using small particle size of seed (Run 160). [P(DMAEMA-*co*-ST) domain was stained with RuO_4]…… 74

4.16 TEM photographs of P(DMAEMA-co-ST)/PMMA composite particles using various crosslinking agent types of seed; (a) Seed: Run 158. DVB: 10 %w/w (Run 221), (b) Seed: Run 159. EGDMA: 5%w/w (Run 222). [P(DMAEMA-*co*-ST) domain was stained with RuO_4]…… 76

4.17 SEM photograph of cationic PST particles (Run 301)……. 77

4.18 SEM photographs of the P(DMAEMA-*co*-ST)/PMMA/PST particles prepared by heterocoagulation for various concentrations of SDS: (a) 0.1 g (Run 403); (b) without SDS (Run 404)…… 80

4.19 TEM photographs of P(DMAEMA-*co*-ST)/PMMA/PST composite particles using various morphology of seed particles; (a) Seed: Run 217, (b) Seed: Run 218, (c) Seed: Run 221, (d) Seed: Run 222, (e) Seed: Run 223. [P(DMAEMA-*co*-ST domain was stained with RuO_4]…… 82

LIST OF FIGURES (continued)

FIGURE PAGE

4.20 SEM photographs of P(DMAEMA-*co*-ST)/PMMA/PST composite particles using various crosslinking agent types of P(DMAEMA -*co*-ST) seed; (a) Seed: Run 158. DVB: 10 %w/w (Run 412), (b) Seed: Run 159. EGDMA: 5%w/w (Run 413)……. 84

ABBREVIATIONS

DMAEMA	dimethyl aminoethyl methacrylate
ST	styrene
MMA	methyl methacrylate
EGDMA	ethylene glycol dimethacrylate
DVB	divinylbenzene
PDMAEMA	poly(dimethyl aminoethyl methacrylate)
P(DMAEMA-*co*-ST)	poly[(dimethyl aminoethyl methacrylate)-*co*-styrene]
PMMA	poly(methyl methacrylate)
PST	polystyrene
AIBN	2,2'-azobisisobutyronitrile
V-50	2,2'-azobis(2-amidinopropane)dihydrochloride
KPS	potassium persulfate
PEO23	poly(oxyethylene nonylphenylether) with 23 units of ethylene oxide
CTAC	cetyltrimethyl ammonium chloride
SDS	sodium dodecyl sulfate
PVP	polyvinylpyrrolidone
MST1	toluene diisocyanate with two poly(ethylene oxide-*b*-propylene oxide-*b*-ethylene oxide) chains
PVA	poly(vinyl alcohol)
EA	ethyl acetate
T_g	glass transition temperature
d_p	mean diameter of polymer

CV	the coefficient of variation
R_i	the rate of initiation
F	the function of the initiator efficiency
k_d	the initiator decomposition constant
[I]	the initiator concentration
IPA	iso-proply alcohol
SEM	scanning electron microscopy
TEM	transmission electron microscopy

CHAPTER I

INTRODUCTION

1.1 Scientific Background and Rationale

Multi-layered polymer particles are used as a component of an emulsion paint and formed into a film coating, since the multi-layered polymer particles have interfaces between core and shells which have largely different refractive indices of light, and as a result, light scattering occurs, and the opacity and shielding property of the coat increase.

The present invention relates to a multi-shell emulsion particle which is useful as an additive to coating compositions for paints, paper coating and information recording papers. The emulsion particles are also useful for heat-sensitive recording materials. Further, the emulsion particles affect weight saving and improves hardness, abrasion resistance and thermal resistance [1].

Recently, acrylate latex containing amino groups has been used as a polymeric crosslinking agent of latices with epoxy groups, to reduce the release of harmful components into the environment, and to enhance the properties of water and solvent resistance and the mechanical strength of the films formed from the latices [2].

However, highly hydrophilic polymers are not easily prepared by conventional polymerization. Dispersion polymerization might give monodisperse microspheres but the polymerization is apt to leave stabilizers in the medium, which would be a harmful contaminant in their applications [3-4]. The hydrophilic homopolymer may flocculate copolymer particles and coagulate the latex.

The synthesis of multi-layered polymer particles consists of three main procedures. The core particles of PDMAEMA copolymer were prepared by emulsion polymerization. Various microspheres of PDMAEMA copolymer with different sizes depend on the composition of recipe. Second, the shell polymer particles were prepared by seeded emulsion polymerization of PDMAEMA core particles with methyl methacrylate (MMA). Refractive index of PDMAEMA (1.4) is smaller than that of PMMA (1.45). Finally, the outer shell polymer particles may be obtained by seeded emulsion polymerization of PDMAEMA/PMMA seeds with ST monomer. The refractive index of PST (1.5) is bigger than PMMA. For three-component emulsion polymer systems, many different structures can be formed [5].

1.2 Objectives of Research Work

1. To synthesize a new type of the multi-layered polymer beads
2. To evaluate their application for scattering UV emission

1.3 Scopes of Research Work

In this research work, the focus is the synthesis of new kinds of multi-layered latex polymers with UV scattering property using the hydrophilic PDMAEMA as the core. The necessary process to achieve the goal may be as follows.

1. Literature survey and in-depth study of this research work.
2. Synthesizing the core of dimethyl aminoethyl methacrylate (DMAEMA) by various polymerization techniques as the following.

   2.1. dispersion polymerization method

2.1.1 The effect of solvent type

2.1.2 The effect of solvent composition

2.2. Suspension polymerization method

2.2.1 The effect of crosslinking agent

2.2.2 The effect of ethyl acetate concentration

2.2.3 The effect of electrolyte concentration

2.2.4 The effect of co-monomer type

2.2.5 The effect of solvent type

2.2.6 The effect of polymerization temperature

2.2.7 The effect of stabilizer type

2.2.8 The effect of styrene content in monomer

2.3. Emulsion polymerization method

2.3.1 The effect of cetyltrimethyl ammonium chloride (CTAC) concentration

2.3.2 The effect of initiator type

2.3.3 The effect of crosslinking agent type

2.3.4 The effect of 2,2'-azobis(2-amidinopropane)•2HCl (V-50) concentration

3. Synthesizing the shell of methyl methacrylate (MMA) by seeded emulsion polymerization

3.1 swelling method

3.2 drop-by-drop method

3.2.1 The effect of initiator type

3.2.2 The effect of particle size of the seed

3.2.3 The effect of the type of crosslinking agent of the seed

4. Synthesizing the outer shell of styrene (ST) by two method

    4.1 Heterocoagulation method

        4.1.1 Synthesizing the cationic small polystyrene (PST) emulsion

        4.1.2 Preparing anionic large PDMAEMA/PMMA particles.

            4.1.2.1 The effect of SDS concentration

        4.1.3 Blending the cationic PST emulsion from Step 4.1.1 in anionic PDMAEMA/PMMA particle by drop-by-drop method

    4.2 Seeded emulsion polymerization method

        4.2.1 The effect of different morphologies of P(DMAEMA-*co*-ST)/PMMA composite particles

5. Characterizing of all steps by

    5.1 Conversion by gravimetrical method

    5.2 Scanning electron microscopy (SEM)

    5.3 Light scattering

    5.4 Transmission electron microscopy (TEM)

    5.5 Differential scanning calorimetry (DSC)

    5.6 Molecular weight by Gel Permeation Chromatography (GPC)

    5.7 Refractive index (RI)

1.4 Contents of Research Work

This thesis consists of 5 chapters. The first chapter deals with the background, the interest and the scope of this research work. Chapter 2 provides the theory of dispersion, suspension, and emulsion polymerizations, composite latex particle morphology and optical properties. Chapter 3 is the experimental part that described

about chemicals, equipment, apparatus and procedure for important parameters of reaction investigated in this work. The results and discussion are explained in Chapter 4 wherein the effects of various reaction parameters on particle size, size distribution, morphology, and refractive index are elucidated and discussed in detail. Finally, the conclusions and suggestion are in Chapter 5.

CHAPTER II

THEORY AND LITERATURE REVIEW

2.1 Dispersion Polymerization

The size of microspheres obtained by dispersion polymerization ranges from submicron to several micrometers. This method can provide microspheres with a very narrow size distribution and can be used for various monomers from hydrophobic to hydrophilic monomers by choosing suitable solvent or a mixture of solvents. Because the monodispersed microspheres with several micrometers are difficult to obtain by emulsion, miniemulsion, microemulsion, and conventional suspension polymerization, this method is very attractive and was largely developed during the last decade. The polymerization mechanism is shown schematically in Figure 2.1. Quite different from the other methods, the initial system is a homogeneous phase composed of a monomer, an initiator, an organic medium, which should be a good solvent for the monomer, but a poor solvent for formed polymer, and a stabilizer which should show affinity (both) to the medium and the formed polymer. After the temperature is raised, the initiator decomposes to generate radicals to which the monomer adds successively in the solvent. After the growing polymer chain reaches a critical length, it precipitates from the medium and becomes a primary nucleus. As in the case of the homogeneous nucleation mechanism in emulsion or emulsifier-free polymerization, the primary nuclei coagulate to a stable one (growing particle) which is stabilized by the stabilizer. Then the growing particles absorb

monomers and capture oligomeric radicals and primary nuclei formed in the medium, and the polymerization site shifts to the growing particles from the continuous phase.

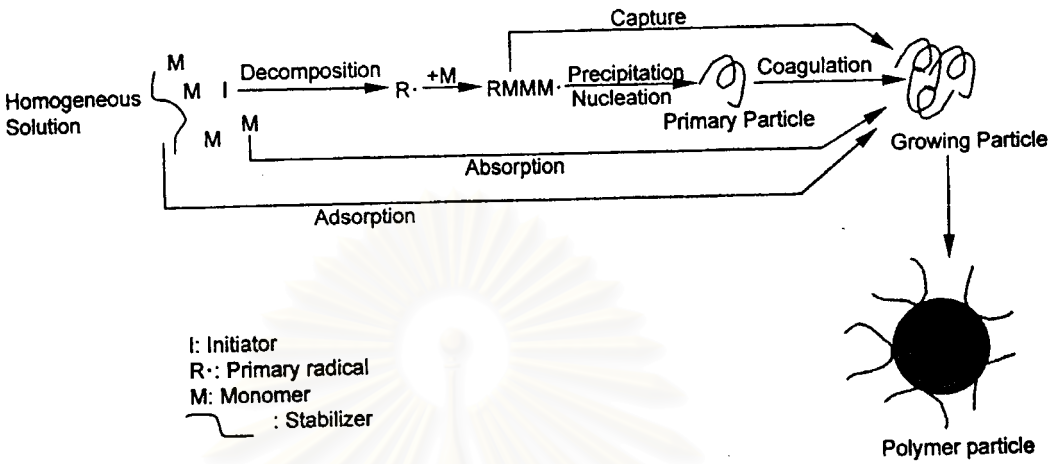

Figure 2.1 Schematic homogeneous nucleation mechanism in dispersion polymerization.

This method has some features in common with homogeneous nucleation of emulsion polymerization or emulsifier-free polymerization. All of them involve a nucleation process, a coagulation process of primary nuclei, and a growing process of the monomer-polymer particles. The nucleation process is complete within the initial stage (about 10 wt% of monomer conversion), and the nuclei are allowed to grow for a long period. However, the critical length of the oligomer at which the primary nuclei precipitate from the medium in dispersion polymerization is longer than that in emulsion polymerization, because organic solvent instead of water is used in the dispersion polymerization. Usually, the compatibility of an organic solvent with a polymer is better than water for allowing a longer oligomer to be dissolved in the solvent. This is also the reason why large microspheres were obtained in the dispersion polymerization, compared to emulsion polymerization [6].

2.2 Suspension Polymerization

Suspension polymerization is a system in which monomers are suspended as the discontinuous phase of droplets in a continuous phase and polymerized. One or more water-insoluble monomers containing oil-soluble initiators are dispersed in the continuous aqueous phase by a combination of strong stirring and the use of small amounts of suspending agents (stabilizers). Suitable conditions of mechanical agitation are maintained while the monomer droplets are slowly converted from a highly mobile liquid state, through a sticky syrup-like dispersion (conversion 20-60%), to hard solid polymer particles (conversion > 70%). The stabilizers hinder the coalescence of the monomer droplets first, and later stabilize the polymer beads whose tendency to agglomerate may become critical when the polymerization has advanced to the point where the polymer beads become sticky.

The most important issue in the practical operation of suspension polymerization is the control of the final particle size distribution. Suspension polymer particle diameters range usually between 50 and 2000 μm, the exact size depending on the monomer type, the concentration of stabilizer, and the agitation conditions in the reactor. These particles are much larger than those formed in emulsion polymerization (20-1000 nm). The particle morphology is an important characteristic for the application of the polymer product, particularly in the case of expandable polystyrene and ion-exchange resins.

In suspension polymerization, size and size distribution of droplets are controlled by stirring speed and the concentration of stabilizer. Therefore, the size distribution of obtained microspheres is very broad. However, because the process is simple and various functional substances can be incorporated into microspheres easily

just by mixing them in the dispersed phase, this method is still a well-established method in the industrial field [7].

The drawback of broad size distribution of suspension polymerization was overcome to a certain extent by improving the dispersing equipment. Omi et al. [8] has recently developed an SPG (Shirasu Porous Glass) emulsification process combined with a subsequent polymerization process to prepare fairly uniform microspheres. The SPG membrane is a porous glass membrane with very uniform pores, consisting of the hydrophilic substance SiO_2-Al_2O_3.

2.3 Emulsion Polymerization

Emulsion polymerization is a most typical and well-known polymerization method for preparing uniform polymeric microspheres composed of relatively hydrophobic monomers. The monodispersed microspheres with diameters from several tens to hundreds of nanometers can be obtained easily by this technique. The polymerization system usually consists of a hydrophobic monomer, water (medium), an emulsifier such as sodium salt of long-chain aliphatic acid, and a water-soluble initiator. The polymerization procedure is as follows. After the monomer is dispersed into the aqueous phase where the emulsifier is dissolved, nitrogen gas is introduced to replace oxygen in the reactor. Then, the temperature is elevated to a desired reaction temperature. Finally, the initiator is added to the system to start polymerization. The advantage of the emulsion polymerization is that the polymerization rate is fast and the size distribution of the obtained particles is very narrow. When the concentration of the emulsifier is above the critical micelle concentration (CMC), the emulsion polymerization of the hydrophobic monomer is

well described by the micellar nucleation mechanism (Harkins' theory), as schematically presented in Figure 2.2.

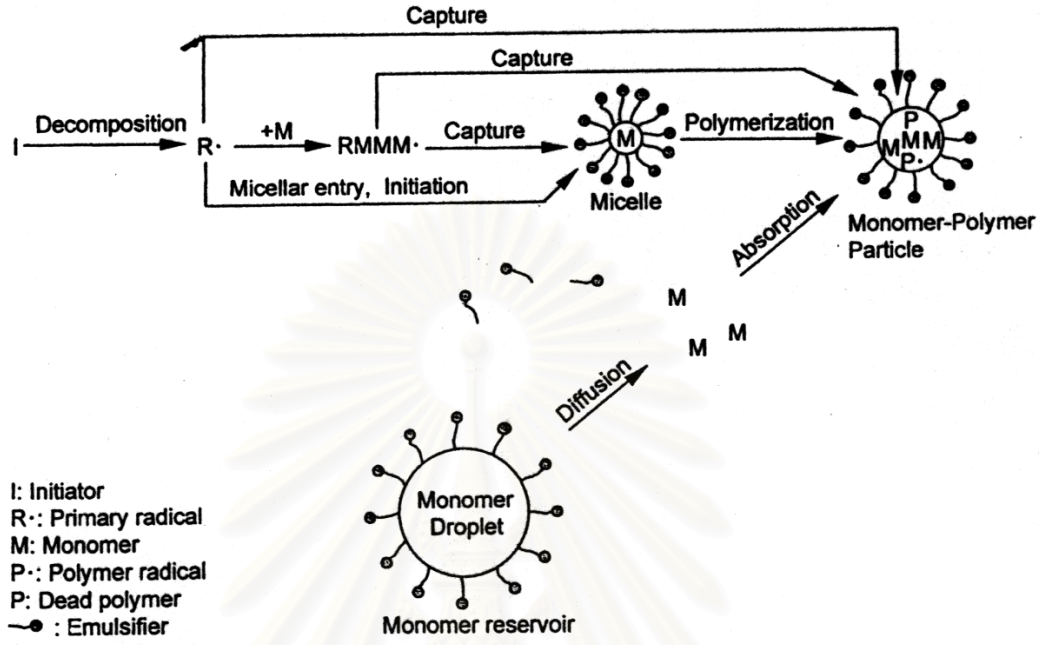

Figure 2.2 Schematic micellar nucleation mechanism (Harkin's theory) in emulsion polymerization.

The polymerization proceeds in three stages: in the first stage, the particles are generated from the monomer-swollen micelles by radicals entering into the micelles from the aqueous phase. After the depletion of the micellar form of emulsifiers, the formation of new particles ends (at about 10% of conversion). In the second stage, the particles grow by means of diffusion of the monomer from the monomer droplets until the monomer droplets disappear (at about 50% of conversion). In the last stage, the particles consume the remaining monomer inside until the complete monomer conversion. Because the formation of the particles ends within a short period and the particles spend a long time to grow, the emulsion polymerization mechanism yields a narrow size distribution of polymer particles [9].

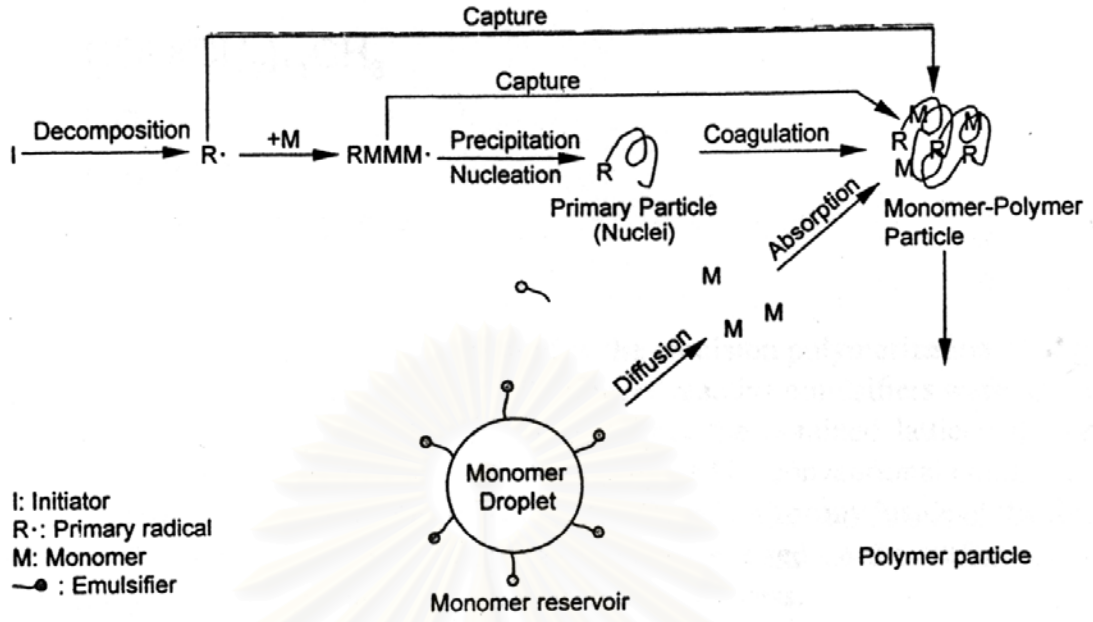

Figure 2.3 Schematic homogeneous nucleation mechanism in emulsion polymerization.

Contrary to the above micellar nucleation theory, the homogeneous nucleation theory is considered to be more applicable to relatively hydrophilic monomers such as methyl methacrylate (MMA) and vinyl acetate (VAc), especially when the emulsifier is below the CMC. As presented schematically in Figure 2.3, this theory assumes that the initiation of polymerization starts in the aqueous phase through the decomposition of the initiator into primary radicals, followed by the addition of monomers dissolved in water. The growth of the oligomeric radical proceeds in the aqueous phase up to a particular critical chain length. On exceeding this critical chain length, the oligomeric radical precipitates from the aqueous phase and forms a water-insoluble polymer in the form of a spherical particle (primary particle, nucleus). The primary particles are unstable and they will coagulate to a large stable particle, which is stabilized by adsorbing emulsifiers of by the ionic charge of initiator fragments on the surface of

the particle. The subsequent growing process of the particle is similar to that of the micellar nucleation process; that is, the growing particle absorbs monomers, which diffuse through the aqueous phase from the monomer droplets to carry out polymerization. The monomer-polymer particle becomes the only polymerization locus.

2.3.1 Role of limited aggregation in particle nucleation

Limited aggregation plays a major role in particle formation in surfactant-free emulsion polymerizations for monomers having a low water-solubility (such as styrene), as well as in emulsion polymerizations with low to moderate emulsifier concentrations and using monomers with higher water-solubility (e.g., methyl methacrylate and vinyl acetate), and emulsion copolymerizations in the presence of water-soluble functional monomers (e.g., acrylic acid, itaconic acid, and sodium styrene sulfonate). This is usually reflected in the presence of a maximum in the number of particles during the early stages of the colloidally unstable primary particles formed by micellar or homogeneous nucleation. The degree of stability of these particles depends on their size, surface charge density, electrolyte valency and concentration, and temperature. Upon aggregation of the primary particles, rearrangement of the physically or chemically bound surface functional groups will occur and thus the particle surface charge density will increase. At a certain size, these particles will acquire a sufficiently high surface charge density to maintain their colloidal stability, and thus further coagulation ceases [10].

2.4 Composite Latex Particle Morphology

2.4.1 Preparation of Composite Particle Structure

Core-Shell Particle Structure

The core-shell particles are usually prepared by a series of consecutive emulsion polymerization sequences with different monomer types, where the second stage monomer is polymerized in the presence of seed particles. The seed particles may be prepared in a separate step, or formed in situ during the emulsion polymerization. The resulting particles are commonly referred to as “core-shell” particle, implying a particle structure with the initially polymerized polymer located in the center of the particle and the later formed polymers becoming incorporated into the outer shell layer.

The formation of a unique multi-layered heterogeneous structure can be expected. Depending on the polymerization process variables, seeded suspension polymerization reaction can produce structured particles, which exhibit a wide variety of particle morphologies such as the familiar core-shell, hemispherical particles with various fragmented inclusions, or “inverted” core-shell particle with the second stage polymer becoming incorporated at the centre of the particles and the seed polymer found on the periphery of the composite particle [11].

2.4.1.1 Seeded Emulsion Polymerization

Seeded polymerization is a potential technique for preparing various functional polymeric microspheres. The system is composed of seed particles, medium, an initiator, monomer droplets, and occasionally, a swelling agent and a stabilizer. After the swelling process is complete, the polymerization is performed.

The seed particles can be of an origin from among the above methods; the medium and initiator should be selected according to purpose. By seeded polymerization, enlarged microspheres, composite, and irregular-shaped microspheres can be obtained by selecting a suitable monomer, initiator, and medium.

Seeded polymerization is composed of 2 steps.

1. Preparation of the seed particles by emulsion polymerization of the first monomer.

2. Addition of the second monomer to the seed particle from stage 1 by seeded emulsion polymerization for a formation of the shell layer onto the seed particle.

This process was performed in three ways.

1. Swelling Polymerization

The equilibrium swelling process, in which the second monomer was allowed to swell the seed particle until the swelling equilibrium is attained. Then the polymerization is performed.

2. Drop-by-drop Polymerization

The semi-batch process, in which the second monomer was added continuously to the reaction flask from a microfeeder.

3. One-Stage Polymerization

The batch process, in which the monomer was added to the reaction flask just before the seeded emulsion polymerization was, initiated [12].

The formation of composite particle can be run by one-stage polymerization. The system of reaction is composed of two monomers, a medium, an initiator, and a stabilizer, which was occasionally agitated at a high speed in the same time before polymerization was initiated. The composite particle is achieved when two monomers are assumed to differ in the reactivity ratio and hydrophilic property.

2.4.1.2 Heterocoagulation

When particles of the same or different sizes but of opposite electrical charge are mixed together, then association of the particles can occur; the resulting effects are referred as heterocoagulation. The particles can be composed either of the same material, e.g. polystyrene, or of different polymers. Moreover, small particles can also heterocoagulate with large particles if they have the same sign of charge and the surface potentials are in the right ranges.

The influence of particle number concentrations on the stability of binary particulate mixtures, at a constant added electrolyte concentration, has been examined by Cheung using a turbidimetric technique to measure the stability ratio of heteroparticle dispersions in a similar manner to that used for homoparticle dispersions.

When heterocoagulation occurs various results can be obtained. For example, Figure 2.4(b) shows schematically that when particles not very different in size but with different charges are mixed in the right ratio, extensive coagulums can be formed. On the other hand, when small particles of one charge are mixed in excess in terms of number concentration with larger particles of the opposite sign, then complete coverage of one particle by the others can occur, as shown in Figure 2.4(a).

A number of aspects of heterocoagulation have become important for the preparation of polymer colloids. Two examples are the growth of particles on to a seed particle in a second-stage emulsion polymerization and the formation of particles of complex morphology, e.g. core-shell particles with the core and shell of different polymers.

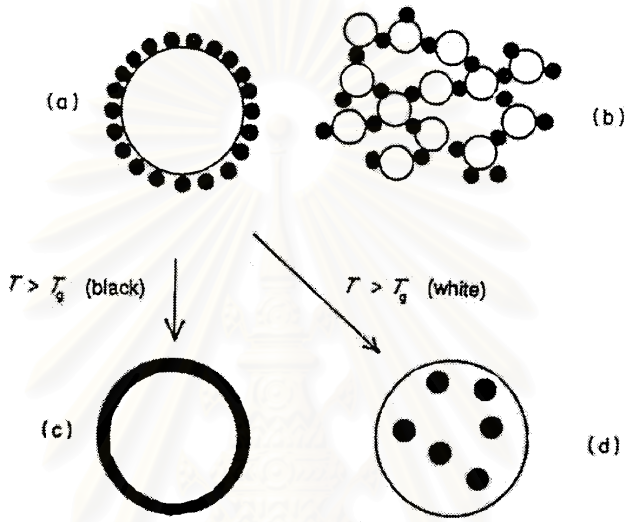

Figure 2.4 Heterocoagulation: (a) surface coating by small latex particles; (b) network formation; (c) encapsulation; (d) engulfment.

As shown in Figure 2.4(a) heterocoagulation provides a possible mechanism for transferring one polymer to the surface of another polymer colloid particle or to the surface of any other type of particle. Once this stage is reached then surface energy considerations becomes important and provided the correct conditions can be achieved, then either the surface particles can be induced to form a shell on the large particle, or the surface particles can be engulfed by the larger one [13].

More recently it has been demonstrated that heterocoagulation can be used as an initial stage in order to achieve either engulfment or encapsulation as illustrated in Figure 2.4(c) and 2.4(d).

2.5 Important Polymerization Parameters in Controlling Particle Morphology

2.5.1 Effect of Polymer/Water Interfacial Tension and Particle Surface Polarity

The most important property of an interface is its interfacial tension, which depends on the molecular interactions between the boundary polymer phase, which is swollen with the second-stage monomer. The outermost layer of a latex particle is different from its interior (core), being enriched with polar groups of different origins, which are better solvated by water, and thus tend to concentrate near the water phase.

2.5.2 Effect of Surfactant

The interfacial tension of the polymer phases against water, which contained surfactant, was in good agreement with the observed particle morphologies. The phase with the higher polymer-water interfacial tension was engulfed by the phase with lower polymer-water interfacial tension.

2.5.3 Effect of Mode of Monomer Addition

In a batch mode of monomer addition, relatively low viscosities are achieved. This enhances the polymer chain mobility, and therefore the migration of the two immiscible polymers in different domains. In semi-batch polymerizations where the second-stage monomer is added continuously to the seed latex at a controlled feed rate, the monomer concentration in the particles can be maintained at a minimal value. The extremely high local viscosity creates a kinetic barrier towards polymer chain diffusion and decreases the degree of phase separation. Semi-continuous monomer addition is one of the widest used methods to control the particle morphology in

industrial applications and to obtain the desired composite particle morphology in cases where thermodynamically non-equilibrium morphologies are desirable.

2.5.4 Effect of Polymer Crosslinking Agents

Another method which is used to increase the kinetic barrier to phase inversion and creates more stable non-equilibrium morphologies is to introduce crosslinking in one or in both of the polymer phases [14].

2.6 Optical Properties

2.6.1 Refractive Index

If a ray of light is incident on a transparent body at an angle α with respect to the normal to its surface, it passes inside the body and continues to travel at a different angle γ with respect to the normal: the light is refracted. The ratio of the sine of the incident beam to the sine of the refracted beam is defined as the refractive index. It equals the ratio of light velocities c_o in vacuum and c in the body according to Snellius' law:

$$n = \sin\alpha/\sin\gamma = c_o/c \qquad (2.1)$$

The Lorentz-Lorenz equation

$$(n^2 - 1) / (n^2 + 2) = 4\pi N\beta / 3V = 4\pi N_A\rho\beta / 3M \qquad (2.2)$$

Polarizabilities $\beta = \mu/E$ depend on dipole moments and applied electric field strength E. Refractive indices thus increase with increasing number and mobility of electrons per molecule.

Carbon atoms have therefore larger polarizabilities than hydrogen atoms. Since the contribution of the latter can be neglected, most organic polymers have refractive indices of ca. 1.5. Exceptions to this rule exist for polymers with especially strong polarizabilities (e.g., fluorine atoms) or with very large pendant groups (e.g., N-carbazole). Even such exceptional molecules still have very similar molecular structures with respect to polalizabilities; the refractive indices of all organic polymers are between ca. 1.33 and ca. 1.73. They vary with the wavelength of incident light [15].

2.6.2 Total internal reflection

Figure 2.5 shows a number of rays diverging from a point source P in a medium of refractive index n and striking the surface of a second medium of refractive index n', where n>n'. From Snell's law,

$$\sin \phi' = n/n' \sin \phi \qquad (2.3)$$

Since n/n' is greater than unity (i.e., $\phi' = 90^o$) for some angle ϕ less than 90^o. This is illustrated by ray 3 in the diagram, which emerges just grazing the surface at an angle of refraction of 90^o. The angle of incidence for which the refracted ray emerges tangent to the surface is called the critical angle and is designated by ϕ_c in the diagram. If the angle of incidence is greater than the critical, the sine of the angle of refraction, as computed by Snell's law, is greater than unity. This may be interpreted to mean that beyond the critical angle the ray does not pass into the upper medium but is totally internally reflected at the boundary surface. Total internal reflection can

take place only when a ray is incident on the surface of a medium whose index is smaller than that of the medium in which the ray is travelling.

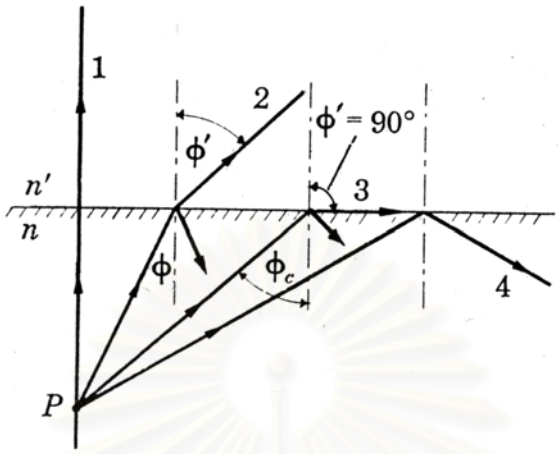

Figure 2.5 Total internal reflection. The angle of incidence ϕ_c, for which the angle of refraction is 90^o, is called the critical angle.

2.6.3 Light Transmission and Gloss

Some of the light incident on a homogeneous, transparent body is reflected from the surface (external reflection) and some passes inside, where it is reflected at an interior boundary of the body (internal reflection). According to Fresnel, the ratio of the intensity I_r of reflected light to the intensity I_o of the incident light depends on both the angle of incident, α, and the angle of reflection, γ :

$$R = I_r / I_o = \tfrac{1}{2} [\sin^2 (\alpha - \tilde{\gamma})(\sin^2 (\alpha + \gamma) + \tan^2 (\alpha - \tilde{\gamma})\tan^2 (\alpha + \gamma)] \qquad (2.4)$$

The reflection R is small for low angles of incidence and begins to increase sharply at high α. If the light enters an optically homogeneous, plane-parallel body perpendicular to its surface, both α and γ become zero and the reflexion reduces to

$R_o = (n- 1)^2 /(n+1)^2$. The light transmission (transmittance) is therefore:

$$\tau_i = 1- R_o = 1- (n- 1)^2 /(n+1)^2 \quad (2.5)$$

Since refractive indices vary only between 1.33 and 1.73, maximum transmittances can only be between 98.0% (n = 1.33) and 92.8% (n = 1.73). These ideal transmittances are rarely obtained since some light is always absorbed or scattered. The most transparent polymer is poly(methyl methacrylate) (n = 1.492); but even PMMA has a transparency of only 93% instead of 96.1% for wavelengths between 430 nm and 1110 nm [15].

Industry defines gloss as ratio of reflection R of the specimen to the reflection R_{st} of a standard which is a specimen with n_D = 1.567 in the paint industry. Gloss R/R_{st} thus increases with increasing refractive index. Theoretical glosses are rarely achieved, however, since surfaces are always somewhat rough and scatter light.

2.7 Literature Reviews

Balakrishnan et al. [16] studied the particle size distribution of suspension copolymers of styrene, chloromethylstryrene, and divinybenzene with gelatin and poly(diallydimethylammonium chloride) as suspension stabilizers which could be varied widely by variation of the relative amounts of monomer and aqueous phases, the stirring speed, and the amount of added anionic surfactant sodium dodecylbenzenesulfonate.

Okay et al. [17] investigated phase separation in polymer beads produced by suspension copolymerization of styrene-divinylbenzene (DVB) with di-2-ethylhexyl phthalate (DOP) as diluent using equilibrium swelling, swelling rate, apparent

densities, and mercury porosimetry. The prepared copolymer in the absence of DOP is heterogeneous, showing that a phase separation exists in the polymerization system, and, in the presence of DOP, the propagating copolymer separates earlier. Furthermore, with increasing amounts of DVB, phase separation occurred earlier than gelation, which caused a sudden increase in the amount of pores about 200-500 °A in diameter corresponding to the interstices between the microspheres.

Someya et al. [18] studied a multi-shell emulsion particle of dry state structure having one or more of penetrating pores connecting the surface layer of the particle with the interior of the particle and having a particle diameter of from 0.1 to 5.0 μm preferably from 0.1 to 1.2 μm. The particle could be prepared by carrying out emulsion polymerization of a vinyl monomer (a) containing from 5 to 80% by weight of an unsaturated carboxylic acid to obtain a polymer (A), forming a polymer (B) in the presence of a particle consisting of the resulting polymer (A) while adding a vinyl monomer (b) in an amount of 10 times by weight or less and at a rate of 3 times by weight per hour or more for the weight of the polymer (A) , and treating the resultant multi-shell emulsion polymer with an alkaline material to neutralize and swell the polymer (A) ; or, after the neutralization treatment, further forming a polymer (C) by adding and emulsion-polymerizing a vinyl monomer (c) in an amount of 20 times by weight or less for the total weight of the polymer (A) and polymer (B). The emulsion particle is useful as a component of resin compositions for paints, paper coating and heat-sensitive recording materials.

Pavinec et al. [19] studied the primary structure of the modifier and the properties of the blend on dependence on a shear stress intensity. They compared the properties of polymer materials prepared from a multilayer poly(methyl methacrylate)

core, butyl acrylate copolymer interlayer, and methyl methacrylate copolymer shell particles {P[MMA-(BAC-co)-(MMA-co)]} by pressmolding from powder and from polymer obtained by stirring a melt of this powder in the chamber of a Brabender mixer (200^{o}C, 60 rpm, 10 min). The powder was obtained from latex by coagulation after polymer synthesis in emulsion. Tensile testing showed different responses of the particle polymers when crosslinked in the middle layer by diallylphthalate (DAP) or by triallylcyanurate (TAC). Although many of the properties of the samples with DAP were improved by kneading, the presence of TAC in polymer particles led mostly to less desirable properties.

Yabuta et al. [20] studied the type of polymeric dispersant of nonaqueous polymer dispersions (NAD) in the performances of the coatings both in liquid paint and in dried films. In the development of NAD coatings for automotive metallic finish, NADs, which were stabilized with acrylic dispersants, were the most useful because the acrylics had a large degree of freedom in modulating the molecular weight, T_g, solubility parameter and the functional groups of the dispersant polymer. The NADs obtained were easily combined with various kinds of solution polymers and crosslinkers, which would form the continuous phase of the coating. The miscibility between the dispersant and the continuous phase polymers was an important factor and should first be considered when selecting NADs to formulate them in the coating. Also, acrylic dispersants were easy to use for modulating the miscibility by changing the monomer composition.

Canche-Escamilla et al. [21] studied polymers of butyl acrylate-methyl methacrylate with different morphologies synthesized by emulsion polymerization. Four types of polymers were obtained: copolymer, core-shell, three layers, and a core-

shell with a copolymer layer of variable composition (gradient). The effect of the morphologies on the mechanical and rheological properties of these polymers was studied. It was found that when the same overall composition was used the properties of the polymer could be varied from those of rigid plastic to those of an elastomeric material. It was also found that increasing the content of butyl acrylate (BA) improves the mechanical properties and the presence of a copolymer zone improves the impact resistance of the material.

Olayo et al. [22] studied the interfacial tension of the water-(PVA)/styrene system measured as a function of the poly(vinyl alcohol) (PVA) concentration and temperature. Average size and particle-size distribution were obtained for a suspension of styrene in water using PVA as a stabilizer.

Okubo et al. [23] studied micron-sized monodispersed PMMA/PST (PMMA/PST = 2/1, wt ratio) composite particles consisting of PMMA-core and PST-shell produced by seeded dispersion polymerization of styrene in a methanol/water medium in the presence of about 2 μm-sized monodispersed PMMA particles. From the viewpoint of thermodynamic equilibrium, such a morphology is difficult to form by usual seeded polymerization in a polar medium such as water. It is concluded that seeded dispersion polymerization in which almost all monomers and initiators exist in the medium has an advantage to produce core/shell polymer particles in which polymer layers accumulate in their order of the production regardless of the hydrophobicity of polymers, because of high viscosity in polymerizing particles.

Kirsch et al. [24] reported on the synthesis of nearly monodisperse phase-separated polymer latices with a well-defined core-shell morphology. Styrene/diisopropenylbenzene and *tert*-butyl acrylate/ethylene glycol-diacrylate were used for either the core or shell of the composite microgel particles. A major concern of the paper is the detailed characterization of the core-shell and inverse core-shell particles by static and dynamic light scattering, transmission electron microscopy, solid-state NMR, and the analytical ultracentrifuge. The effect of the cross-linking agent on the final phase-separated morphology is discussed and compared with theoretical predictions.

Omi et al. [25] proposed a two-step polymerization process to obtain composite latices with an average size ranging from submicrons to 1 μm. Negatively changed PMMA seed latex particles were prepared by using anionic sodium lauryl sulfate (SLS), and ammonium persulfate (APS). After the removal of unreacted monomer and initiator by dialysis, seeded emulsion polymerization was carried out by swelling the PMMA seeds with monomers consisting of hydrophilic DMAEMA and hydrophobic styrene. A cationic initiator, 2,2'-azobis(2-amidinopropane)•HCl (V-50), was used. A small amount of non-ionic polyoxyethylene nonylphenyl ether (POE23) solution was added. The weight percent of DMAEMA in co-monomer, weight ratio of monomer to polymer (M/P), and pH of the latex were changed to obtain controlled coagulation and further growth of the seed particles. Incorporation of DMAEMA was investigated by TEM observation of the particles stained with iodomethane, and by measuring the rate of quarternization of DMAEMA when iodomethane gradually diffused into the particles from the continuous phase. A maximum growth of the particles, from the initial average diameter of 0.21 μm to a

final 0.56 μm, was attained when pH was set at 10.0 with a lower POE23 concentration. The final particles were stable aggregates of the several seed particles with DMAEMA incorporated between the coagulated seeds as well as deposited on the particles. The nucleation of DMAEMA-rich secondary particles was enhanced when the pH was set at 9.0. Decreasing the amount of POE23 normally promoted the growth unless the stability of the latex was affected.

Jonsson et al. [26] studied latex particles containing equal amounts of poly (methyl methacrylate) (PMMA) and polystyrene (PST) prepared by polymerizing styrene in the presence of PMMA seed particles using two different initiators, potassium persulfate (KPS) and *tert*-butyl hydroperoxide (*t*-BHP). Styrene was added either before polymerization (batch) or continuously during the polymerization. Particles prepared using batch addition of styrene showed no signs of a core-shell morphology, and the surface concentration of PST was lower than 50%. Particles with well-defined core-shell structures were obtained when styrene was added at a low feed rate. With *t*-BHP as initiator, the shell layer was compact and distinct and the surface concentration of PST high, whereas with KPS as initiator the shell layer was thicker and contained domains of PMMA. Composite particles prepared using a low styrene feed rate, but seed particles containing a chain-transfer agent, had PST domains distributed throughout the entire particle volume. Hence, the formation of particles with a core-shell structure was due to the suppression of radical transport to the interior of the seed particles, mainly because of the high internal viscosity of the latter. The structure and composition of the shell layer, however, depends on the chemical nature of the initiator.

Chen et al. [27] derived a thermodynamic analysis and a mathematical model to describe the free energy changes corresponding to various possible morphologies in composite latex particles. Seeded batch emulsion polymerization was carried out at 70^{o}C using seed monodisperse polystyrene latex particles having different surface polarity. Methyl methacrylate and ethyl methacrylate were polymerized in a second stage seeded emulsion polymerization using polystyrene particles as seed in the presence of a nonionic stabilizer, nonyphenol polyethylene oxide (Igepal Co-990). Two types of initiators, potassium persulfate ($K_2S_2O_8$) and azobisiobutyronitrile (AIBN), were used to change the interfacial tension between the second stage polymer (in monomer) and water interface. The results showed that, rather than the polymer bulk hydrophilicity, the surface particle polarity is the controlling parameter in deciding which phase is inside or outside in the composite particle. The predicted morphologies showed good agreement with the observed particle morphologies of the composite latices.

Lee et al. [28] found that when hydrophobic monomers are polymerized in the presence of highly hydrophilic polymer seed particles, the second-stage hydrophobic polymers form cores surrounded by the first-stage hydrophilic polymers, resulting in inverted core-shell latices. The formation of core-shell morphology by this inversion process has been found to be dependent on the hydrophilicity and molecular weight of the first-stage hydrophilic polymers and the extent of phase separation between the two polymers involved. Particle morphology has been examined by electron microscopy, surface acid titration, alkali swelling of particles and surface reactivity.

Cho et al. [29] prepared poly(methyl methacrylate)-polystyrene composite particle latices by poly(methyl methacrylate)-seeded emulsion polymerization of styrene employing batch, swelling-batch, and semibatch methods, The changes in particle morphology taking place during the polymerization reaction were followed by electron microscopy. Anchoring effect exerted by ionic terminal groups introduced by ionic initiator was found to be the main factor in controlling the particle morphology. The polymer particles obtained by oil-soluble hydrophobic initiators such as azobisisobutyronitrile and 4,4'-azocis-(4-cyanovaleric acid) gave the inverted core-shell morphology. Water-soluble hydrophilic initiator, $K_2S_2O_8$, also gave the inverted core-shell morphology. However, in this case the occurrence of the halfmoonlike, the sandwichlike, and the core-shell morphologies were also observed depending upon the polymerization conditions. The distribution of terminal $-SO_4^-$ groups on the surface area of polystyrene particles could be controlled by initiator concentration and polymerization temperature.

Ma et al. [30] studied monodispersed crosslinked cationic poly(4-vinylpyridine-co-butyl acrylate) [P(4VP-BA)] seed latices prepared by soapless emulsion polymerization, using 2,2'-azobismethyl(propionamidine)dihydrochloride (V-50) as an initiator and divinylbenzene (DVB) or ethylene glycol dimethacrylate (EGDMA) as a crosslinker. The optimum condition to obtain monodispersed stable latex was investigated. It was found that the colloidal stability of the P4VP latex can be improved by adding an adequate amount of BA (BA/4VP = ¼, w/w), and adopting a semi-continuous monomer feed mode. Subsequently, poly(4-vinylpyridine-co-butyl acrylate)/Poly(styrene-co-butyl acrylate) [P(4VP-BA)/P(ST-BA)] composite microspheres were synthesized by seeded polymerization, using the above latex as a

seed and a mixture of ST and BA as the second-stage monomers. The effects of the type of crosslinker, the degree of crosslinking, and the initiators (AIBN and V-50) on the morphology of final composite particles are discussed in detail. It was found that P(4VP-BA)/P(ST-BA) composite microspheres were always surrounded by a PST-rich shell when V-50 was used as initiator, while sandwich-like or popcorn-like composite particles were produced when AIBN was employed. This is because the polarity of the polymer chains with AIBN fragments is lower than that of the polymer with V-50 fragments, hence leading to higher interfacial tension between the second-stage PST-rich polymer and the aqueous phase, and between PST-rich polymer and P4VP-rich seed polymer. The zeta potential of composite particles initiated by AIBN in seeded polymerization shifted from a positive to a negative charge.

Okubo et al. [31] proposed the blend emulsion of two kinds of polymer particles, in which almost all of the cationic soft small particles (SPs) were adsorbed onto the anionic hard large particles (LPs) by utilizing a stepwise heterocoagulation method. The blend emulsion was cast to a micro-heterogeneous film. In the film, LPs played a discontinuous phase and SPs with a content of 30 wt% played a continuous one as film forming additives. The storage stabilities of the blend emulsions after the stepwise heterocoagulation were examined under various conditions, and the morphology of the film was estimated from the attenuated total reflectance Fourier-transform infrared spectroscopy.

Kemmere et al. [32] studied the influence of recipe and process conditions on the coagulation behavior of polystyrene (PST) and polyvinyl acetate (PVAc) latices. Seeded batch experiments reveal a significant influence of electrolyte concentration

on the coagulation behavior of both PS and PVAc latices. Within the experimental error, no dependency of the coagulation behavior on process conditions, in terms of energy dissipation, reactor scale, impeller type, and impeller diameter, has been observed for the reactor scales investigated. These results indicate that intrinsic chemical influences such as electrolyte concentration dominate the coagulation behavior during emulsion polymerization.

Shiozaki et al. [33] prepared a new technique to control the triboelectric charge (TEC) of polymer microspheres. Polymer microspheres (PMs) were prepared by three-component suspension copolymerization of styrene (ST), 2-ethylhexyl methacrylate (EHMA) and dimethylaminoethyl methacrylate (DMAEMA). Emulsion particles (EPs) for surface modification were prepared by emulsifier-free three-component emulsion copolymerization of ST, EHMA, and sodium styrene sulfonate (NaSS). PMs were covered with EPs by a process similar to the 'stepwise heterocoagulation technique'. The value of TEC of modified microspheres varied from –30 μC/g to –60 μC/g with increasing NaSS content of EPs from 3wt% to 6wt%, though unmodified particles had small values of TEC. This fact suggests that the surface modification by the above procedure can lead to the preparation of particles having a desired TEC.

Okubo et al. [34] prepared composite polymer emulsion particles which consist of two kinds of polymer by seeded emulsion polymerization. In general, there are few situations in which the two polymers are completely mixed. Therefore, during polymerization the phase separation of polymers occurs in the particles and polymer particles with different heterogeneous structures are formed at the end of the

process according to the polymerization conditions. They are interested in this polymer mixing process in microparticles with diameters in the range 0.1-1.0 μm because the properties of films cast from such composite polymer emulsions were clearly varied corresponding to the morphology of particles, even if the polymer compositions are same. In addition, in those polymerizations they observed some anomalous particles, e.g., confettilike, raspberrylike, and void particles.

Muroi et al. [35] studied the progressive dissolution of carboxylated latex particles with increasing pH utilized to investigate the internal structure of core-shell latex particles, in comparison with that of copolymeric latex particles formed from the same monomers. The results indicated that for particles formed by two-stage feed polymerization from both ethyl acrylate (EA) – methacrylic acid (MAA) and methyl acrylate (MA)-MAA mixtures, a core-shell morphology consisting of a poly(MA-MAA) shell with a comparatively high MAA content and a core composed of both poly(MA-MAA) and poly(EA-MMA). In contrast, the particles formed by two-stage polymerization of an MA-EA-MAA mixture exhibited a fairly uniform ratio of MA/EA content from surface to center. Examination of the distribution of the carboxylic groups in all of the latex particles showed their concentration to be highest at the surface and to decrease with proximity to the center.

Kada et al.[36] demonstrated that a photochemical reaction can create various distributions of refractive index in polymer. When the polymer containing a photochemically active material is irradiated by UV light, the photochemical reaction which breaks the π-conjugated system in the material and decreases its linear polarizability can reduce refractive index of the polymer. They prepared a PMMA

film incorporating DMAPN ((4-N, N-dimethylaminophenyl)-N'-phenylnitrone) with a ratio of 23 wt% by spin coating. Electronic structural change of DMAPN and refractive index of the film before and after UV irradiation were evaluated by UV absorption spectra and m-line method, respectively. The UV irradiation decreased λ_{max} at 380 nm in the absorption spectra, which is attributed to nitrone, and the refractive index decreased exponentially with irradiation time. The change of refractive index reached 0.028. The refractive index profile upon depth of the film was investigated by measuring refractive index of stacked DMAPN/PMMA films. When UV with a power of 10.7 mW/cm^2 was irradiated upon three stacked DMAPN/PMMA films for 35 s, variation of the refractive index change showed a quadratic profile. The refractive index profile with various irradiation times can be accounted with the combination of the chemical kinetics with the steady state approximation and Lambert-Beer's law. Thus, the photochemical reaction can be used to control the refractive index distribution in polymer.

Ulrich et al. [37] used the prism coupler to determine the refractive index and the thickness of a light-guiding thin film known from experiments on integrated optics. Both parameters are obtained simultaneously and with good accuracy by measuring the coupling angles at the prism and fitting them by a theoretical dispersion curve. The fundamentals and limitations of this method are discussed, also its practical use, and mathematical procedures for the evaluation.

CHAPTER III

EXPERIMENTAL

3.1 Chemicals

3.1.1 Monomer

Dimethyl aminoethyl methacrylate (DMAEMA, Wako Pure Chemical Co., Japan), methyl methacrylate (MMA), and styrene (ST) from Kishida Chemical Industries Co. Ltd., Japan were of commercial grade. They were each distilled under reduced pressure, and stored in a refrigerator prior to use.

3.1.2 Initiator

2,2'-Azobisisobutyronitrile (AIBN, Wako Pure Chemical Industries Co. Ltd., Japan) was used as a hydrophobic initiator for the suspension polymerization and dispersion polymerization; while 2,2'-azobis(2-amidinopropane)•2HCl (V-50) and potassium persulfate (KPS) (Wako Pure Chemical Co., Japan) were used as hydrophilic initiators for the emulsion polymerization and seeded emulsion polymerization. They were of reagent grade and used as received.

3.1.3 Suspending Agent

Poly(oxyethylene nonylphenylether) with 23 units of ethylene oxide (PEO23) and polyvinylpyrrolidone K30 (PVP, M_V 40,000) were used as stabilizers for the suspension polymerization. Cetyltrimethyl ammonium chloride (30 wt% CTAC, Kao Chemicals Co., Japan) and sodium dodecyl sulfate (SDS, Merck Co.,

Germany) were used as stabilizers for the emulsion polymerization. Methacryloyl-terminated PMMA (AA-6) macromonomers, toluene diisocyanate with two poly(ethylene oxide-*b*-propylene oxide-*b*-ethylene oxide) chains (MST1), polyvinylpyrrolidone K30 (PVP, M_V 40,000), and poly(vinyl alcohol) (PVA-217, degree of polymerization 1700, degree of hydrolysis 88.5%) provided by Kuraray Chemical Co., Ltd. (Osaka) were used as stabilizers for dispersion polymerization.

3.1.4 Crosslinking Agent

Ethylene glycol dimethacrylate (EGDMA) and divinylbenzene (DVB), containing 55% active isomeric DVB, 40% ethyl vinylbenzene, and 5% saturated hydrocarbons, from Kishida Chemical Industries Co. Ltd., Japan were of commercial grade. They were washed with 5%w/w Na_2CO_3 solution, then with water, and dried with 4^oA molecular sieve. They were stored in a refrigerator prior to use.

3.1.5 Solvents

Ethyl acetate (EA) and acetone (Kishida Chemical Industries Co. Ltd., Japan) were of commercial grade and distilled prior to use for suspension polymerization. Toluene, 1-butanol, 2-butanone, acetonitrile, and iso-butanol were purchased from Kishida Chemical Industries Co. Ltd. (Japan) and distilled prior to use for dispersion polymerization.

3.1.6 Other Chemicals

Hydrochloric acid (35% HCl, Wako Pure Chemical Co., Japan) was used for pH adjustment of the aqueous phase for suspension polymerization. Sodium sulfate (Na_2SO_4, Wako Pure Chemical Industries, Japan) was used as an electrolyte for

emulsion polymerization in the first stage. Potassium chloride (KCl, Kanto Chemical Co., Japan) was of reagent grade used as an electrolyte for heterocoagulation in the final stage. 2-Propanol or isopropyl alcohol (IPA, Kishida Chemical Industries Co. Ltd., Japan) was of commercial grade and distilled prior to use for heterocoagulation.

3.2 Glassware

3.2.1 Four-necked round bottom flask 500 cm^3

3.2.2 Reflux condenser

3.2.3 Thermometer

3.2.4 Nitrogen gas tube

3.2.5 Other general laboratory glassware

3.3 Equipment

3.3.1 Scanning Electron Microscopy (SEM) : Jeol JSM-6400, Tokyo, Japan

3.3.2 Transmission Electron Microscopy (TEM) : Hitachi H-700, Japan

3.3.3 Zeta Potential : Microtech Nichion Sony Zeecom, Japan

3.3.4 Differential Scanning Calorimetry (DSC) : Netzch 200, Germany

3.3.5 Light Scattering : Zetasizer 1000HS, Malvern Instruments, England

3.4 Polymerization Procedures

The process of synthesis of composite PDMAEMA/PMMA/PST can be divided into three stages.

3.4.1 Preparation of PDMAEMA Core Particles

3.4.1.1 Dispersion Polymerization

A typical run was prepared as follows. A solution containing 10 g of DMAEMA, 0.5 g of PEO23, 0.2 g of AIBN, and 90 g of a water/iso-butanol solvent mixture (50/50 wt%) was weighed into a 250 cm^3 flask. The mixture was deoxygenated by bubbling nitrogen gas for 1 h and subsequently heated to the reaction temperature at 343 K in 30 min. The polymerization was carried out for 18 h.

3.4.1.2 Suspension Polymerization

The mixture of distilled water, EA, PEO23, and 2 N HCl was used as the continuous phase. DMAEMA and the co-monomer were mixed in the continuous phase in a reactor. During the nitrogen bubbling the agitation was continued at room temperature for 1 h and the flask was subsequently heated to the reaction temperature at 343 K in 30 min. After 5 cm^3 of the initiator solution had been slowly added at a rate of 3 $cm^3 min^{-1}$, the polymerization was carried out for 24 h.

In order to obtain a seed latex free of EA, the seed latex was stripped with nitrogen gas at about 313 K for 12 h or until no odor of EA was detected.

3.4.1.3 Emulsion Polymerization

PDMAEMA seed particles were synthesized at 343 K for 12 h. The synthetic procedure was the same as that for suspension polymerization except that the initiator solution was added immediately (10 $cm^3 min^{-1}$) in the reactor.

3.4.2 Preparation of PMMA Shell by Seeded Emulsion Polymerization

3.4.2.1 Swelling Method

The swelling was carried out as follows: the seed latex and MMA monomer are charged to a 500 cm^3 four-necked round-bottom reactor connected with a semicircular anchor-type blade for agitation, dimrhoth condenser, and nitrogen inlet nozzle. The nitrogen gas was gently bubbled into the latex for 1 h. The nozzle was then lifted above the latex surface and the mixture was heated to 343 K.

3.4.2.2 Drop-by-Drop Method

The PDMAEMA copolymer seed latices were put in a 500 cm^3 four-necked round-bottom reactor connected with a semicircular anchor-type blade for agitation, a dimrhoth condenser, and a nitrogen inlet nozzle. The nitrogen gas was gently bubbled into the latex for 1 h. The nozzle was then lifted above the latex surface and the temperature was increased to 343 K. The initiator solution free of oxygen was added immediately. Ten grams of MMA were slowly added at a rate of 0.17 $cm^3 min^{-1}$ to the reactor over approximately 1 h and polymerized for 6 h.

3.4.3 Preparation of PST Outer Shell

3.4.3.1 Heterocoaggulation

Heterocoagulation of cationic PST and anionic P(DMAEMA-*co*-ST)/PMMA was carried out stepwise as follows:

3.4.3.1.1 Preparation of Cationic PST Emulsion

The distilled water, ST, and CTAC were charged to a 500 cm^3 four-necked round-bottom reactor equipped with stirrer, condenser, thermometer,

and nitrogen inlet tube. After passing nitrogen gas through the mixture for 1 h, the mixture was heated to 333 K. After V-50 solution had been immediately added to the reactor, the polymerization was carried out for 4 h.

Ten grams of cationic PST emulsion was diluted with water to 5 %wt solid and mixed with KCl and IPA.

3.4.3.1.2 Preparation of Anionic P(DMAEMA-*co*-ST)/PMMA Particles

The P(DMAEMA-*co*-ST)/PMMA seed particles, KCl, IPA and SDS were mixed in a 150 cm^3 beaker.

3.4.3.1.3 Blend Emulsion by the Stepwise Heterocoagulation Method

The cationic PST and anionic P(DMAEMA-*co*-ST)/PMMA emulsions were blended at the PST/[P(DMAEMA-*co*-ST)/PMMA] ratio of 20/80 (w/w) at 323 K.

3.4.3.2 Seeded Emulsion Polymerization

P(DMAEMA-*co*-ST)/PMMA/PST composite particles were synthesized at 343 K for 8 h. The synthetic procedure was the same as that for preparing PMMA shell by drop-by-drop method. All the polymerizations involved the use of the different seeds.

3.5 Characterization

3.5.1 Conversion

After the polymerization, the final monomer conversions of PDMAEMA copolymer by dispersion, suspension and emulsion polymerization were measured by

gravimetry. Polymers in a weighed latex sample were precipitated by acetone, centrifuged, washed two times, dried in a vacuum oven and weighed. The conversion was calculated according to the following equation (3.1):

$$conversion\ (\%) \quad = \quad \frac{w_1}{w_0} \Big/ \left(\frac{W_1}{W_0} \right) \times 100, \qquad 3.1$$

where w_1, w_0,W_1, W_0, are the weights of the dried polymer latex, sample, fresh monomer, and reaction mixture, respectively. The result was obtained as an average value from two measurements.

The monomer conversions of PDMAEMA/PMMA and PDMAEMA/PMMA/PST composite polymers prepared by seeded emulsion polymerization were measured by gravimetry. Two milliliters of latex were centrifuged and followed by decantation of the supernatant, then dried in a vacuum and weighed. The conversion of composite polymers was calculated according to the following equation (3.2):

$$conversion\ (\%) \quad = \left(\frac{w_1}{w_0} \Big/ \frac{W_1}{W_0} \quad - \frac{W_s}{W_1} \right) \times 100, \qquad 3.2$$

where W_s is the weight of the seed polymer latex.

3.5.2 Scanning Electron Microscopy (SEM)

The external morphologies of PDMAEMA copolymer, PDMAEMA/PMMA, and PDMAEMA/PMMA/PST composite polymer and the size and size distribution of PDMAEMA copolymer were observed by scanning electron microscopy (SEM, SM-35CF II-A, JEOL, Japan). The specimens were prepared by

dilution of polymer latex. Diluted latex was dropped on an aluminium film adhered on the stub. The specimens were coated with a thin layer of gold under reduced pressure using a fine coater JEOL model JFC-1200. The mean particle size and its size distribution of PDMAEMA copolymer prepared using suspension polymerization were determined by a direct measurement of 200 particles per sample on SEM photos.

3.5.3 Light Scattering

The size and size distribution of P(DMAEMA-*co*-ST) copolymer obtained by emulsion polymerization, P(DMAEMA-*co*-ST)/PMMA, and P(DMAEMA-*co*-ST)/PMMA/PST composite polymer by the seeded emulsion polymerization were observed by light scattering method (Zetasizer 1000HS, Malvern Instruments Ltd. England).

3.5.4 Transmission Electron Microscopy (TEM)

The morphologies of PDMAEMA/PMMA and PDMAEMA/PMMA/PST composite polymers were observed by transmission electron microscropy (TEM, Model H-700, Hitachi, Japan). The TEM specimens were prepared according to a similar procedure by Ma [38], ultrathin films were cut from the particles embedded in epoxy resin with an RMC MT-7000 ultramicrotome (Atom Tech Ltd., England) and were set them on the copper meshes. The PST domain was stained by exposing the specimens to the vapor of an aqueous RuO_4 solution (0.5%) for 90 min in a sealed bottle at room temperature.

3.5.5 Thermal Properties of Polymers

Glass transition temperature (T_g) of PDMAEMA copolymer was investigated using a differential scanning calorimeter (Netzch 200, Germany) with a heating rate of 10^{o}C min^{-1} and a cooling rate of 20^{o}C min^{-1}. The sample (8-12 mg) was placed in an aluminium pan and was then put in the sample slot at room temperature along with an empty pan as a reference to assist output balance. For a random copolymer, the T_g is given by Fox equation as a good approximation,

$$\frac{1}{T_{g12}} = \frac{W_1}{T_{g1}} + \frac{W_2}{T_{g2}}, \qquad 3.3$$

where W_1 and W_2 are the weight fractions of monomer 1 and 2, and T_{g1} and T_{g2} are the glass transition temperatures of their corresponding homopolymer.

3.5.6 Gel Permeation Chromatography (GPC)

The average molecular weight (Mw) and molecular weight distribution (MWD) of the PDMAEMA/PMMA and PDMAEMA/PMMA/PST composite polymer particles were obtained using Tosoh GPC model HLCH820. The dried polymer sample of 1 mg was dissolved in 2 cm^3 of THF to an approximate concentration of 0.1 wt%. The filtered polymer solution was injected into the chromatographic column at a flow rate of 0.5 cm^3 min^{-1}.

3.5.7 Zeta Potential

The latex was diluted with ca 500 volume times with DDI water for a measurement of zeta potential. The zeta potential was determined by direct

measurement of the electrophoretic rate of particles in a 45 V direct current field and automatically calculated by the equipment (Microtech Nichion Sony Zeecom).

3.5.8 Refractive Index (RI)

Films for refractive index measurements were prepared by spin coating the polymer solution on a fused-silica plate. Measurement of refractive index of latex was investigated by m-line method [36-37]. The measurement set up is shown in Figure 3.1.

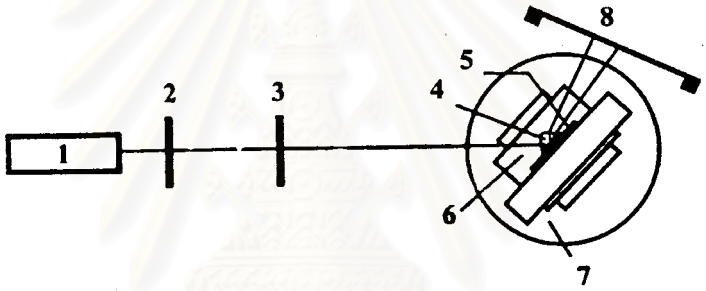

Figure 3.1 M-line method setup: (1) He-Ne laser source (632.8 nm), (2) polarizer rotator, (3) polarizer, (4) prism, (5) film on a fused-silica plate, (6) X-Y stage, (7) rotation state, (8) screen.

CHAPTER IV

RESULTS AND DISCUSSION

4.1 Preparation of PDMAEMA Core Particles

4.1.1 Dispersion Polymerization

4.1.1.1 Effect of Solvent Type

Hydrophilic PDMAEMA particles were prepared by dispersion polymerization using AIBN as an initiator. Various organic solvents were investigated and, among them, a iso-butanol/water mixture was most effective. Methacryloyl-terminated PMMA (AA-6), polyvinylpyrrolidone K30 (PVP), poly(vinyl alcohol) (PVA-217, degree of polymerization 1700, degree of hydrolysis 88.5%), and toluene diisocyanate with two poly(EO-*b*-PPO-*b*-EO) chains (MST1) were used as stabilizers. It was found that the reaction did not require any type of stabilizer in a mixed solvent of iso-butanol and water (50:50 wt%), which produced PDMAEMA particles in the micron range. In the dispersion polymerization, the solvent ratio between good and poor solvents greatly affected the particle size and size distribution. Control of particle size was attempted by varying the ratio between good and poor solvents in the dispersion polymerization of 2-hydroxyethyl methacrylate (HEMA) using poly(styrene-*block*-butadiene) [P(ST-*b*-Bd)] stabilizer. Uniform PHEMA particles in the micron range have been achieved in a mixture of 2-butanol and toluene [39]. We used n-butanol, toluene, and iso-butanol as good solvents for PDMAEMA. The poor solvents employed were 2-butanone, acetonitrile,

acetone, and distilled water. The stable PDMAEMA seed latex particles were crosslinked with 3% (by weight) of ethylene glycol dimethacrylate (EGDMA) based on the total weight of the monomer. The crosslinking agent was employed only in a mixture of iso-butanol and water.

4.1.1.2 Effect of Solvent Composition

The detailed preparation conditions are shown in Table 4.1 by varying the solvent composition between water and iso-butanol of 0:100, 20:80, 30:70, 40:60, 50:50, 55:45, and 70:30 wt% based on total weight of mixed solvent.

Table 4.1 Recipe of P(DMAEMA-*co*-ST) seed particles by dispersion polymerization

Run No.	**7**	**20**	**19**	**18**	**6**	**22**	**8**
Monomer							
DMAEMA (g)	8.7	8.7	8.7	8.7	8.7	8.7	8.7
ST (g)	1.0	1.0	1.0	1.0	1.0	1.0	1.0
EGDMA (g)	0.3	0.3	0.3	0.3	0.3	0.3	0.3
AIBN (g)	0.2	0.2	0.2	0.2	0.2	0.2	0.2
Solvent							
Water (g)	-	18	27	36	45	40.5	63
Iso-butanol (g)	90	72	63	54	45	49.5	27
Conversion (%)	*	*	14	12	16	**	**

Condition: Bubbling N_2 for 1 h, polymerization time of 24 h, * no particles, ** gel-like

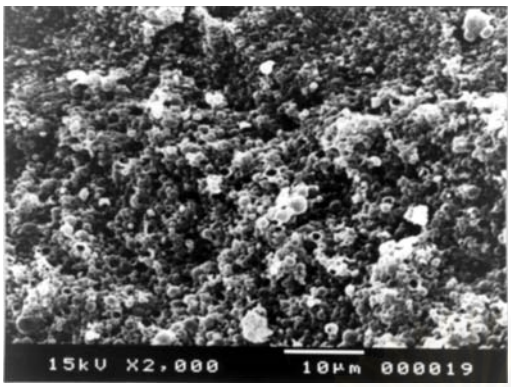

(a)

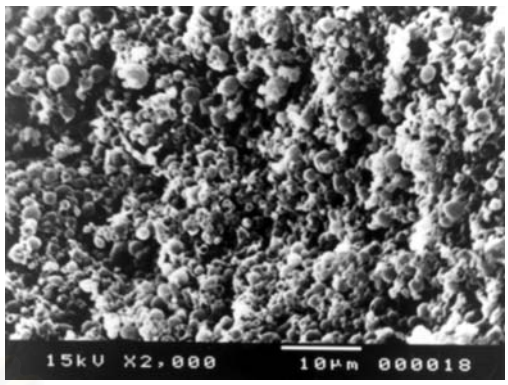

(b)

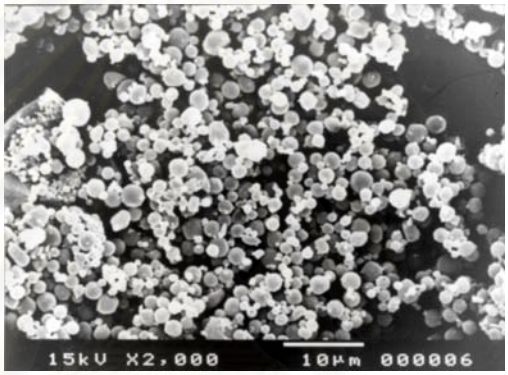

(c)

Figure 4.1 SEM photographs of P(DMAEMA-*co*-ST) particles for various ratios of water to iso-butanol : (a) 30:70 (Run 19), (b) 40:60 (Run 18), (c) 50:50 (Run 6).

The results demonstrate that PDMAEMA microspheres were obtained in the solvent mixture containing 30 to 50% water based on the total weight of mixed solvent. Below 30 wt% of water in a mixed solvent, no particles were obtained. These results indicate that a poor solvent of water is essential for the polymer to precipitate from the mixed solution. Because of the hydrophilic nature of the polymer, the swelling of the PDMAEMA particles of course increased as the content of water increased (> 50 wt%). The polymerization in solvents containing a higher

water content gave smaller PDMAEMA particles (Run 19, 18, and 6) as shown in Figure 4.1, because more phase separation in the system controlled the polymer particle size. In this system, the monomer conversion was less than 30%, as determined by the gravimetric method, and the polymer particles were highly viscous. Therefore, it could be concluded that this system was inappropriate for preparing composite latices with MMA due to the high viscosity, low conversion (lower than 30%), and difficult stripping of iso-butanol (b.p. 381 K) and elimination of unreacted reactants.

4.1.2 Suspension Polymerization

4.1.2.1 Effect of the Crosslinking Agent

EGDMA was used as a crosslinking agent to prevent the dissolution of DMAEMA from the seed particles, inhibit diffusion of the exterior-layer-constituent polymer into the interior of particles, limit swelling in new monomers and increase the glass transition temperature and molecular weight of PDMAEMA particles. Crosslinking latices of PDMAEMA copolymer were easy to apply to substrates [18]. The effect of the crosslinking agent, EGDMA, on the PDMAEMA copolymer morphology was studied, with AIBN dissolved in acetone and EA, and with different types of co-monomers: MMA and ST. Table 4.2 shows the results for PDMAEMA copolymers prepared by suspension polymerization.

The effects of EGDMA on the particle size of the copolymers, P(DMAEMA-*co*-MMA) and P(DMAEMA-*co*-ST), are given in Table 4.2. In the presence of 3 wt% EGDMA (based on the monomer), the crosslinked P(DMAEMA-*co*-ST) and P(DMAEMA-*co*-MMA) latices gave a large amount of coagulum during

Table 4.2. Recipe of PDMAEMA Seed Particles by Suspension Polymerization

Run No.	110	113	115	116	117	119	120	121	126	129	133	134	136	137	144	145
Water (g)	176	176	166	171	176	176	176	176	176	176	176	176	176	176	179	176
PEO23 (g)	4.0	4.0	4.0	4.0	4.0	4.0	4.0	4.0	4.0	4.0	4.0	4.0	4.0	4.0	-	4.0
PVP (g)	-	-	-	-	-	-	-	-	-	-	-	-	-	-	0.5	-
Na_2SO_4 (g)	-	-	-	-	-	-	0.26	0.026	-	-	-	-	-	-	-	-
2 N HCl (g)	1.0	-	1.0	1.0	1.0	1.0	1.0	1.0	-	1.0	1.0	1.0	1.0	1.0	1.0	1.0
0.1 N NaOH (g)	-	-	-	-	-	-	-	-	1.8	-	-	-	-	-	-	-
DMAEMA (g)	17.4	17.4	16.0	15.4	16.0	16.0	16.0	16.0	16.0	16.0	16.0	16.0	16.0	16.0	16.0	10.0
ST (g)	2.0	2.0	-	-	-	-	-	-	-	4.0	4.0	4.0	4.0	4.0	4.0	10.0
MMA (g)	-	-	4.0	4.0	4.0	4.0	4.0	4.0	4.0	-	-	-	-	-	-	-
EGDMA (g)	0.6	0.6	-	0.6	-	-	-	-	-	-	-	-	-	-	-	-
AIBN (g)	0.4	0.4	0.4	0.4	0.4	0.4	0.4	0.4	-	0.4	0.4	0.4	0.4	0.4	0.4	0.4
EA (g)	-	5.0	5.0	5.0	15.0	10.0	5.0	5.0	-	5.0	5.0	5.0	5.0	5.0	5.0	5.0
Acetone (g)	5.0	-	-	-	-	-	-	-	-	-	-	-	-	-	-	-
KPS (g)	-	-	-	-	-	-	-	-	0.4	-	-	-	-	-	-	-
Temp. (K)	343	343	343	343	343	343	343	343	343	343	343	348	338	333	343	343
Conversion	68	88	62	73	68	68	62	65	no latex	64	57	72	72	64	73	87
d_p (μm)	**creased surface**	**coagulum**	**5.37**	**coagulum**	**3.30**	**22.06**	**7.63**	**7.53**	**-**	**1.27**	**8.23**	**agglomerated**	**2.26**	**agglomerated**	**-**	**-**
%CV	**-**	**-**	**26.7**	**-**	**26.1**	**42.9**	**38.6**	**28.7**	**-**	**29.7**	**20.0**	**-**	**33.0**	**-**	**-**	**-**

Bubbling N_2 for 1 h, adding 5 cm^3 AIBN in 2 min., polymerization time of 24 h

the polymerization using AIBN dissolved in EA as illustrated in Runs 113 and 116, respectively. Additionally, the crosslinked PDMAEMA particle aggregates became large enough to be macroscopically visible, differed in density from the surrounding medium and settled quite rapidly, leaving a more or less clear supernatant. As mentioned above, it was concluded that EGDMA provided critical influence on the coagulum particles in suspension polymerization using AIBN dissolved in EA. Much coagulum was formed and precipitated when EGDMA was added. When using acetone as a solvent, crosslinked P(DMAEMA-*co*-ST) particles with in creased surfaces were obtained in Run 110 as shown in Figure 4.2. Figure 4.2 shows interesting morphology because the walls of the polymer particles almost collapsed. This result confirms the finding of Tawonsree et al. [40] who found that an increase in EGDMA concentration resulted in coarser, porous spheres. In the absence of EGDMA, the coagulum disappeared and a stable P(DMAEMA-*co*-ST) latex was obtained using 20 wt% of ST in Run 129, whereas a stable P(DMAEMA-*co*-MMA) latex was not obtained using 20 wt% of MMA in Run 115. The cause of these phenomena is considered to be related to the addition of EGDMA. We can conclude that EGDMA produced coagulum and coarser particles, in suspension polymerization using AIBN both in EA and acetone, resulting from phase separation. As mentioned above, uncrosslinked P(DMAEMA-*co*-MMA) stable latex could not be prepared: a large amount of coagulum was generated during the polymerization while the concentration of DMAEMA was high in the aqueous phase, from which unreacted monomers could be absorbed on the coagulum during polymerization. The uncrosslinked PDMAEMA is rubbery, composed of mostly soft segments of oligomers or monomers, and sticks together easily.

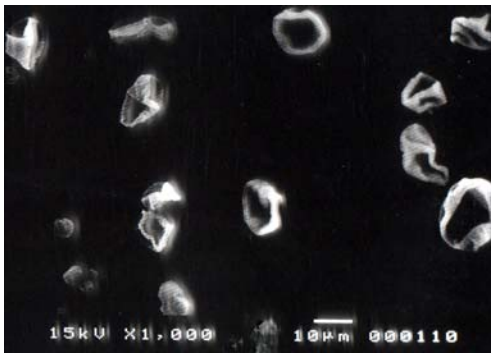

Figure 4.2 SEM micrograph of the crosslinked P(DMAEMA-*co*-ST) particles using AIBN dissolved in acetone (Run 110).

4.1.2.2 Effect of the Ethyl Acetate Concentration

The polymerizations were performed by charging 2.8, 5.8, and 9.0 wt% of EA, respectively, to the continuous phase. The MMA concentration was 20 wt% based on the total weight of the monomer, as shown for Runs 115, 119, and 117 in Figure 4.3. However, uncrosslinked, stable P(DMAEMA-*co*-MMA) latex was not obtained from these experiments due to its hydrophilic copolymer chains. Figure 4.4 shows that the particle size was considerably affected by the addition of EA. The mean particle diameter increased from 5.37 to 22.06 μm when the amount of EA was increased from 2.8 to 5.8 wt%. An exception was found in Run 117 (9.0 wt% of EA), for which the particle diameter did not follow the increasing trend. We consider that this was probably related to the formation of a more homogeneous copolymer composition because of the addition of EA in the continuous phase. The hydrophobicity of copolymer chains increased as the number of MMA units increased. Therefore, the interfacial tension between the continuous phase and the particles increased, and they tended to coagulate to form bigger particles so as to

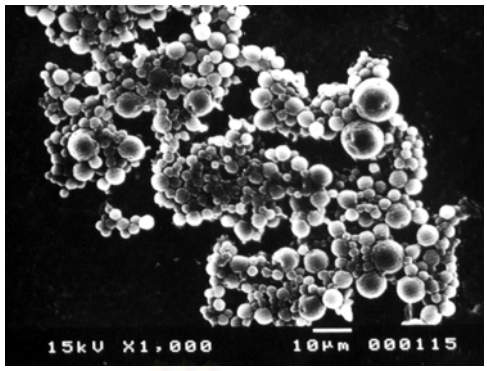

(a)

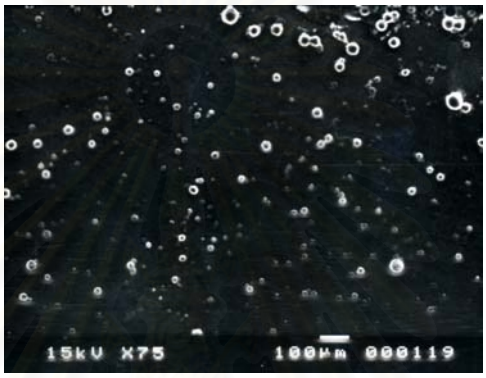

(b)

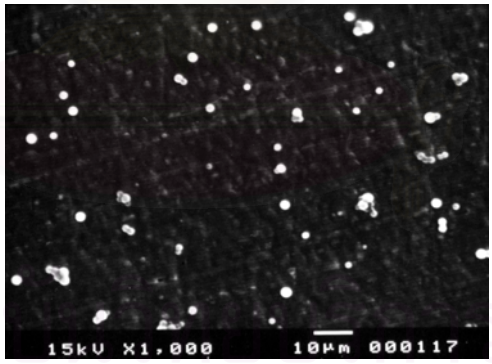

(c)

Figure 4.3 SEM micrographs of the uncrosslinked P(DMAEMA-*co*-MMA) particles for various concentrations of ethyl acetate: (a) 2.8 wt% (Run 115); (b) 5.8 wt% (Run 119); (c) 9.0 wt% (Run 117).

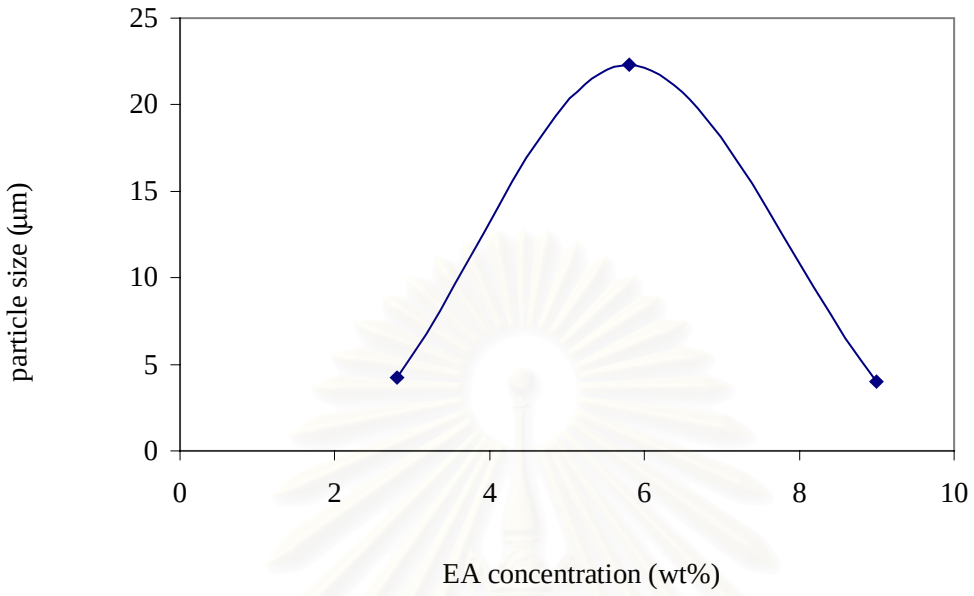

Figure 4.4 Dependence of the particle size of P(DMAEMA-*co*- MMA) on the concentration of ethyl acetate in the continuous phase.

decrease the interfacial tension. The second reason was that the electrostatic repulsion force between the particles decreased as the permittivity of the continuous phase decreased, possibly due to the increase of particle size and the chain transfer behavior of EA in the particles, as the amount of EA was increased. However, when 9.0 wt% of EA was added into the polymerization system, it was found that the particle diameter decreased. The reason for these drastic changes is considered to be changes in the polarity of the continuous phase resulting from the addition of EA, which decreases the solubility of DMAEMA in the water due to the considerable hydrophilicity of PDMAEMA, probably leading to the formation of a hairy layer on the surfaces of microspheres. When the concentration of EA increased in the continuous medium it forced the hairy layer to collapse.

4.1.2.3 Effect of Electrolyte Concentration

The electrolyte, sodium sulfate, was added to stabilize PDMAEMA chains. Sodium sulfate induces charges in the PDMAEMA chains, which are not soluble in water. It has been known that hairy chains collapse with increasing amount of electrolytes due to the compression of electric double layer. This behavior decreases, generally, the particle size and its size distribution. The effects of the electrolyte on the properties of resulting latex are also shown in Table 4.2 which indicates that the particle size, particle size distribution and agglomerated particles were greatly affected by the addition of Na_2SO_4. The mean size of the uncrosslinked P(DMAEMA-*co*-MMA) particles prepared by charging Na_2SO_4 in Run 121 (7.53 μm) was unexpectedly bigger than that without Na_2SO_4 addition in Run 115 (5.37 μm), but agglomerated particles still occurred in both runs. The mean particle size of the uncrosslinked P(DMAEMA-*co*-MMA) particles increased from 7.53 to 7.63 μm

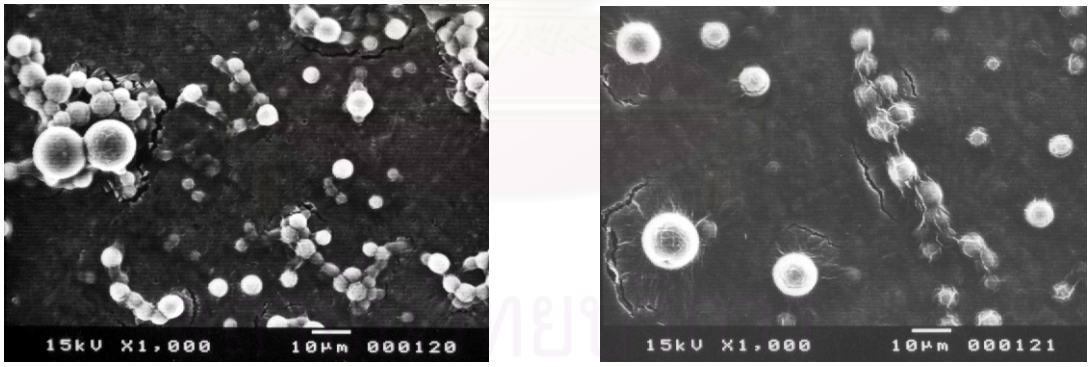

(a) (b)

Figure 4.5 SEM photographs of the uncrosslinked P(DMAEMA-*co*-MMA) particles for various concentrations of Na_2SO_4 electrolyte: (a) 10^{-3} M (Run 121); (b) 10^{-2} M (Run 120).

when increasing the Na_2SO_4 input from 10^{-3} M to 10^{-2} M, and the coefficient of variation increased, from 28.7% to 38.6% in Runs 121 and 120, respectively, as

shown in Figure 4.5. However, the hairy layer model is considered to explain why the mean particle sizes of the uncrosslinked P(DMAEMA-*co*-MMA) increased as the electrolyte concentration increased. This model postulates that the surface of a particle is coated by a layer of flexible polymer chains with terminal ionic groups. These chains can extend into the distant continuous phase, depending on the electrolyte concentration [41].

4.1.2.4 Effect of Co-monomer Type

Hydrophilic MMA (1.5 wt% dissolved in water) and hydrophobic ST were used as co-monomers. Their chemical structures are different, but the glass transition temperatures of both polymers are very similar (T_g of PMMA = 378 K, T_g of PST = 377 K). As shown in Table 4.2, stable P(DMAEMA-co-ST) latex was obtained when charging 20 wt% of ST based on the total weight of monomer. However, stable P(DMAEMA-*co*-MMA) latex was not obtained by charging 20 wt% of MMA based on the total weight of monomer, and the mean particle size of P(DMAEMA-*co*-MMA) in Run 115 (5.37 μm) was found to be greater than that of P(DMAEMA-*co*-ST) in Run 129 (1.27 μm), probably due to the rather hydrophilic copolymer of MMA. In the case of the P(DMAEMA-*co*-MMA), the thickness of the hairy layer increased, due to the increase of PDMAEMA solubility caused by the PMMA moiety. Resulting from its hydrophilicity, the P(DMAEMA-*co*-MMA) particles were stuck together, forming a neck-like or dumbbell-like structure as shown in Figure 4.3(a). The observed T_g values of the uncrosslinked P(DMAEMA-*co*-MMA) and P(DMAEMA-*co*-ST) are shown in Table 4.3. However, both observed T_g values are close to the T_g of randomly copolymerized P(DMAEMA-*co*-MMA) and P(DMAEMA-*co*-ST), which should be in the vicinity of 304 K according to Fox's

equation for the co-monomer DMAEMA-MMA to DMAEMA-ST composition ratio of 8:2. Two T_g values are found in this case, indicating that phase separation occurred in the particles. Second T_g may be from the grafted PEO stabilizer. PEO graft copolymers claimed to act as a bridge that facilicates the transport of the radicals through the interface region at interparticle collision. The grafted PEO on the P(DMAEMA-*co*-ST) as such cannot be removed by a simple washing in acetone. We proposed that the Tg2 could be the transition for the grafted PEO/P(DMAEMA-*co*-ST)

Table 4.3 Glass transition temperature of the PDMAEMA copolymers

Run No.	**$T_{g\ (calc)}$ (K)**	**$T_{g1\ (obs)}$ (K)**	**$T_{g2\ (obs)}$ (K)**
115	303	340.0	428.2
129	304	336.1	436.9
145	327	378.1	430.3

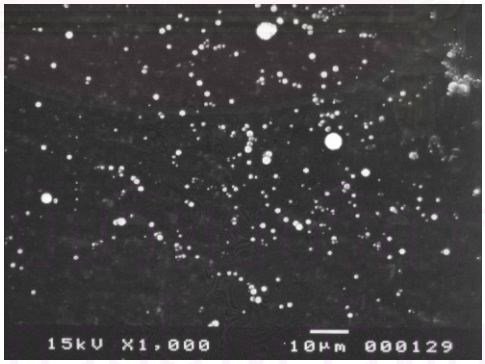

Figure 4.6 SEM photograph of the uncrosslinked P(DMAEMA-*co*-ST) particles using AIBN dissolved in ethyl acetate (Run 129).

4.1.2.5 Effect of Solvent Type

Suspension polymerization of the uncrosslinked P(DMAEMA-*co*-ST) was carried out by a batch operation to select the solvent. The use of AIBN is noticeable because it is slightly soluble in the aqueous phase. It is possible that coagulation occurred because most AIBN was in the hydrophilic monomer phase. AIBN could enter the interface, where a large amount of polar molecules such as water and DMAEMA existed, and the latex was thus obtained as expected. However, the polarity of interfacial layer would easily decrease due to the presence of a good solvent. The addition of organic solvents was considered to dissolve AIBN and decrease the permittivity of the continuous phase. Based on water, 2.8 wt% of EA and acetone were charged. In this work, acetone and EA were selected so as to lower the polarity of the continuous phase and enhance the stability of PDMAEMA particles. As a result, stable latex was prepared by charging 2.8 wt% of EA and acetone to the initiator system as shown in Figures 4.6 and 4.7, respectively. Solvent types with different solubility parameters, such as acetone (δ = 9.9 $MPa^{1/2}$) and EA (δ = 9.1 $MPa^{1/2}$), influence the particle size of the uncrosslinked P(DMAEMA-*co*-ST). Acetone produced uncrosslinked P(DMAEMA-*co*-ST) having mean particle size of 8.23 μm while EA produced 1.27 μm mean particle size. Thus the mean particle size of the uncrosslinked P(DMAEMA-*co*-ST) using acetone (in Run 133) was found to be bigger than when using EA (in Run 129), because the polarity of acetone was stronger.

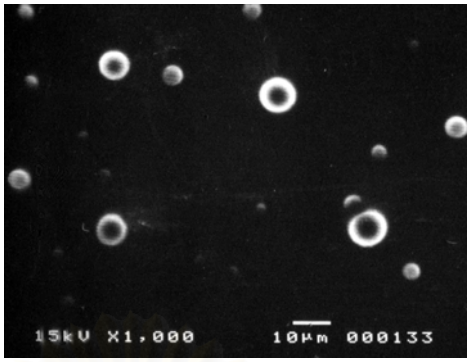

Figure 4.7 SEM photograph of the uncrosslinked P(DMAEMA-*co*-ST) particles using AIBN dissolved in acetone (Run 133).

4.1.2.6 Effect of Polymerization Temperature

The temperature range for copolymerization was from 338 to 343 K as shown in Table 4.2. Agglomerated particles were produced at both 333 K and 348 K reaction temperatures in Runs 137 and 134, respectively. The mean particle size increased from 1.27 to 2.26 μm when decreasing the polymerization temperature from 343 to 338 K in Runs 129 and 136, respectively. The effects of polymerization temperature on the particle size and size distribution are shown in Figure 4.8 (Runs 137, 136, 129, and 134). Bigger particles with a broader distribution (CV = 30%) were obtained when the copolymerization was conducted at a lower temperature. The reasons are probably related to the effects of the reaction temperature on (1) the rate and degree of polymerization and (2) the solubilities of organic compounds. Increasing the reaction temperature usually increases the number of nuclei, the rate of polymerization and chain transfer of polymer radicals, leading to a decrease in particle size of the uncrosslinked P(DMAEMA-*co*-ST). Increasing the reaction temperature generally promotes dehydration of the polyoxyethylene chains of PEO23,

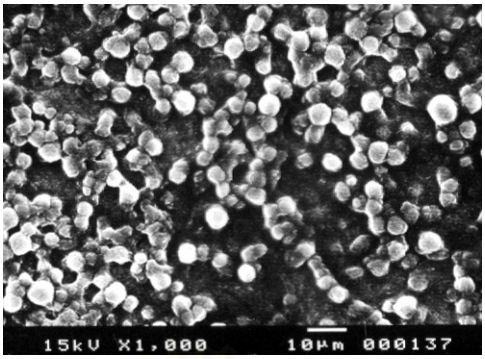

(a)

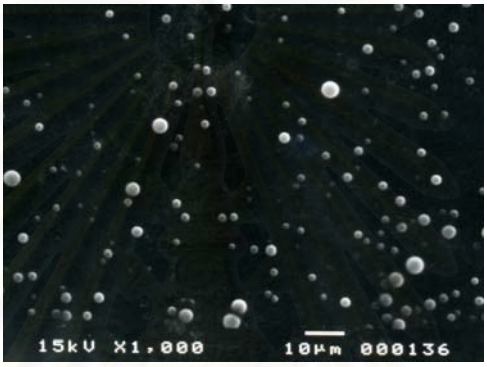

(b)

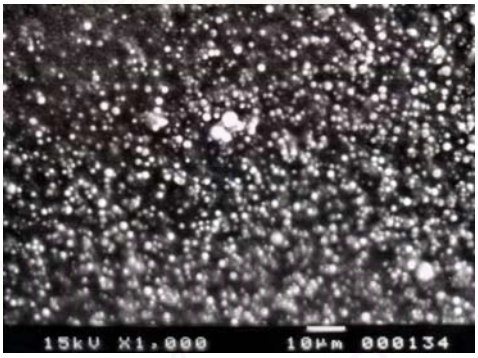

(c)

Figure 4.8 SEM photographs of the uncrosslinked P(DMAEMA-*co*-ST) particles prepared at various polymerization temperatures: (a) 333 K (Run 137); (b) 338 K (Run 136); (c) 348 K (Run 134).

which in turn reduces the monomer solubility [42]. Furthermore, Ni et al. [43] found that the solubilities of 4-vinylpyridine (4VP), EA, and MMA decreased at higher temperatures. The solubility of EA in water is around 8.3 wt% at 298 K, and decreases at higher temperatures (an azeotropic mixture of water 6.1 wt% was formed at 343 K). As mentioned above, this attribute reveals that the particles become smaller due to the decreasing solubility of DMAEMA as the polarity of the continuous phase is getting lower.

In addition, agglomerated particles occurred at 333 K and 348 K, resulting from collisions of particles inducing more agglomeration than the transfer of growing radicals through the cluster to each particle. Each radical is also supposed to be formed from collisions between monomer droplets (particles) saturated with the oil-soluble initiator, AIBN. The concentration of the radical is proportional to the collisions between droplets (particles). The particles are effectively protected by the stabilizer molecules, and the stability of P(DMAEMA-*co*-ST) depends on the amount of stabilizer.

4.1.2.7 Effect of Stabilizer Type

The stabilizer performs the dual function of providing sites for particle nucleation, as well as providing colloidal stability to the growing particles as a result of their adsorption at the particle-water interface. Non-ionic stabilizers are used for controlling latex particle morphology and for enhancing the post-polymerization colloidal stability against mechanical shear, freezing and added electrolytes. In this work, stabilizers were used to decrease the hydrophilicity of the PDMAEMA surface or increase the charge density of the PDMAEMA surface so as to enhance the repulsive force between microspheres. PVP was used as a stabilizer

instead of PEO23, a nonionic stabilizer, because PVP was a good stabilizer for PDMAEMA due to the similarity of nitrogen containing of PVP with those of PDMAEMA ($-NH_2$). Therefore, PVP can better interact with the DMAEMA, providing smaller PDMAEMA particles. The surface active molecules of PVP with an active amino group of PDMAEMA can chemically combine with the stabilizer to the surface of the particles. The diameter of the P(DMAEMA-*co*-ST) particles so obtained using PVP in Run 144 was smaller than that by PEO23 in Run 129 with the same conditions. This seems to be dependent on the type of stabilizer. However, with the addition of the PVP, the particle size of the resultant latex was too small to be observed by SEM.

4.1.2.8 Effect of ST Content in Monomer

Figure 4.9 shows an electron micrograph of uncrosslinked P(DMAEMA-*co*-ST) particles with 50% ST content in the monomer. Due to the greater hydrophobicity of ST in comparison to DMAEMA, stable latex was obtained. The particle size distribution of PDMAEMA does not depend on the amount of ST under the investigated conditions of Run 145 as shown in Table 4.2. Moreover, the particle size distribution of the resultant latex was too broad to be measured on SEM photos. This is because the DMAEMA units in the copolymers are concentrated on the surface of the polymer particles and hence DMAEMA is likely to dissolve in the aqueous phase during the polymerization. However, the glass transition temperature of the uncrosslinked PDMAEMA copolymer increased when the amount of ST was increased. Increasing the ST content from 20 to 50 wt%, based on the total weight of monomer, leads to the calculated T_g of the uncrosslinked P(DMAEMA-*co*-ST) from Fox's equation increasing from 304 K to 328 K. The observed T_g values of

P(DMAEMA-*co*-ST) are shown in Table 4.3. The trends of changing T_g of the copolymers are in agreement with the values calculated from Fox's equation: the increasing ST content raises the T_g in the same direction for the observed and

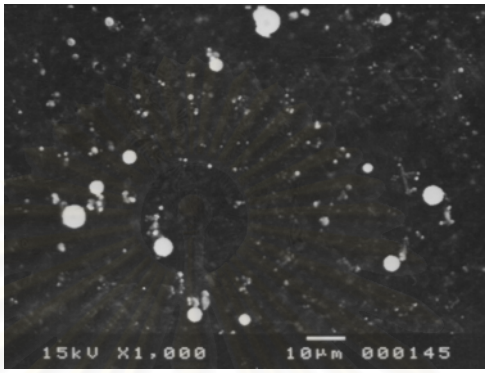

calculated values. Two T_g values are observed in the P(DMAEMA-*co*-ST) latex.

Figure 4.9 SEM photograph of the uncrosslinked P(DMAEMA-*co*-ST) particles with 50% ST content in monomers (Run 145).

4.1.3 Emulsion Polymerization Method

To prepare the cationic P(DMAEMA-*co*-ST) seed particles, 2,2'-azobis(2-amidinopropane)•2HCl (V-50) with a cationic stabilizer was used. Addition of Na_2SO_4 to the continuous phase produced a positive charge on PDMAEMA chains that restricted the chains dimension and stabilized them.

4.1.3.1 Effect of CTAC Concentration

In emulsion polymerization, three particle formation mechanisms, micellar, homogeneous and droplet nucleation, may be operating simultaneously. Which mechanism dominates particle formation depends on the stabilizer concentration, the monomer solubility in the aqueous phase, and the level of subdivision of the monomer droplets [44].

Table 4.4 Recipe of P(DMAEMA-*co*-ST) Seed Particles by Emulsion Polymerization

Run No.	**152**	**153**	**154**	**156**	**157***	**159***	**160**
DMAEMA (g)	16.0	16.0	16.0	16.0	16.0	16.0	16.0
ST (g)	4.0	4.0	4.0	4.0	2.0	3.0	4.0
DVB (g)	-	-	-	-	2.0	-	-
EGDMA (g)	-	-	-	-	-	1.0	-
Water (g)	190	190	190	190	190	190	190
Na_2SO_4 (g)	0.25	0.25	0.25	0.25	0.25	0.25	0.25
CTAC (g)	2.50	0.65	1.30	-	1.31	1.31	1.32
SDS (g)	-	-	-	0.65	-	-	-
V-50 (g)	0.40	0.40	0.40	-	0.40	0.40	1.01
KPS (g)	-	-	-	0.40	-	-	-
Conversion	60	72	76	25	66	67	70
pH	-	9.08	8.84	-	9.64	8.76	9.59
ζ-potential (mv)	-	-56	-87	-	-77	-57	-50
d_p (nm)	64	129	117	**	800/13484	602	47
%CV	25	30	20	-	-	-	18

Agitation rate 120 rpm, bubbling N_2 for 1 h, polymerization temperature 343 K, polymerization time of 12 h

*The latices were filtered to eliminate the coagulum before observing the particle size

** Spherical and non-spherical morphology

In this study, CTAC was employed as a cationic stabilizer in the emulsion copolymerization of DMAEMA and ST. Table 4.4 shows the results for the uncrosslinked P(DMAEMA-*co*-ST) particles using CTAC of 0.65, 1.30, and 2.50 wt% (based on the total weight) in Runs 153, 154, and 152, respectively. It reveals that the amount of CTAC influences the particle size. The results indicate that stability of the copolymerization for the DMAEMA-containing system was obtained when CTAC was used. Comparisons of the particle size obtained with different

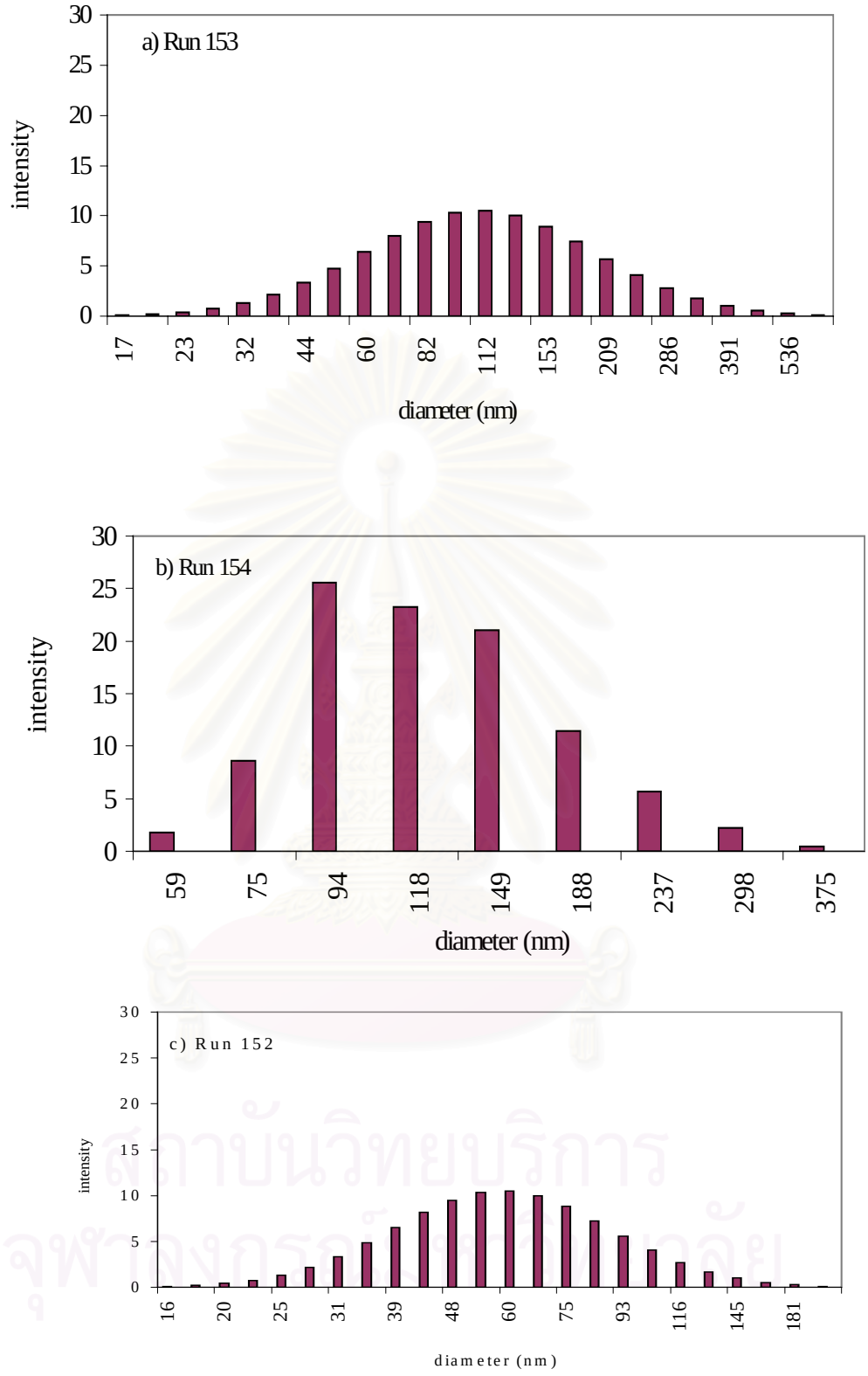

Figure 4.10 Histograms of the size distribution of the uncrosslinked P(DMAEMA-*co*-ST) particles using different concentrations of CTAC: (a) 0.65 wt% (Run 153); (b) 1.30 wt% (Run 154); (c) 2.50 wt% (Run 152)

CTAC concentrations are given in Table 4.4. The mean particle size decreased from 129 to 64 nm when the concentration of CTAC was increased from 0.65 to 2.50 wt%. A particle size histogram for the uncrosslinked P(DMAEMA-*co*-ST) from the concentration effect of CTAC is given in Figure 4.10. The distribution of the particle diameters was roughly from 16 to 600 nm. For concentrations of CTAC at 0.65, 1.30, and 2.50 wt%, the mean particle diameters were around 129, 117, and 64 nm, respectively. The size distribution imposed by the CTAC at a concentration of 1.30 wt% was rather narrow (CV = 20%) and the peak diameters were 95, 117, and 148 nm. The addition of CTAC caused a low interfacial tension between the monomer phase and the water phase. With increasing concentration, the stabilizer decreased the mean particle size and increased the number of particles or the fraction of interface.

4.1.3.2 Effect of Initiator Type

The monomer phase containing DMAEMA and ST in a 80:20 weight ratio was studied with different types of initiators: V-50 and KPS. Uncrosslinked P(DMAEMA-*co*-ST) particles from emulsion polymerization, using SDS as an anionic stabilizer with KPS as an anionic initiator, could be either spherical or non-spherical and the monomer conversion was lower than 30% in Run 156 as shown in Table 4.4. However, no latex was formed using PEO23 as a nonionic stabilizer with KPS in Run 126 as shown in Table 4.2.

While using CTAC as a cationic stabilizer with V-50 as an initiator, the uncrosslinked P(DMAEMA-*co*-ST) particles were stable and the monomer conversion was higher than 60% in these experiments. In the case of using KPS, which is a pure inorganic salt, the initiator should be completely dissolved in the aqueous phase where a majority of DMAEMA existed. There should be no initiator in the monomer phase. In this case, the stable emulsion could not be prepared even

by changing the stabilizer. This result indicates that the formation of latex is related to the place where the initiator exists. On the contrary, V-50 is substantially an organic substance, and both the molecule and the radical derived from V-50 can effectively diffuse to the interface monomer, which is an organic phase. These characteristics have proven to be important for the formation of latex. All the results shown above can explain why V-50 more easily enters the interfacial layer than KPS. The polymerizations are, therefore, faster and conversions are, of course, higher with V-50 than with KPS. This can be explained by one or a combination of the following data: (1) differences in values of the decomposition rate constant of V-50 (343 K; k_d = 1.15 x 10^{-4} l mol^{-1} s^{-1}) and KPS (343 K; k_d = 2.33 x 10^{-5} l mol^{-1} s^{-1}); and (2) electrostatic interactions between microemulsion droplets and the charged radicals [46].

4.1.3.3 Effect of Crosslinking Agent Type

The effect of the crosslinking agent [divinylbenzene (DVB), from Kishida Chemical Co., containing 55% active isomeric DVB, 40% ethyl vinylbenzene, and 5% saturated hydrocarbons; or EGDMA] on the P(DMAEMA-*co*-ST) morphology was studied by emulsion polymerization using V-50 as an initiator. The polymerization recipe and experimental results are summarized in Table 4.4. The crosslinking agent DVB at 10 wt% and EGDMA at 5 wt% based on the monomer were added to DMAEMA-ST co-monomers in Runs 157 and 159, respectively. We found that the addition of the crosslinking agent (EGDMA or DVB) caused a phase separation of the highly crosslinked network from the PDMAEMA. EGDMA-rich copolymers containing -$COOCH_3$ pendant groups were formed in the early stage of the polymerization, because DVB or EGDMA is more reactive than ST and tends to

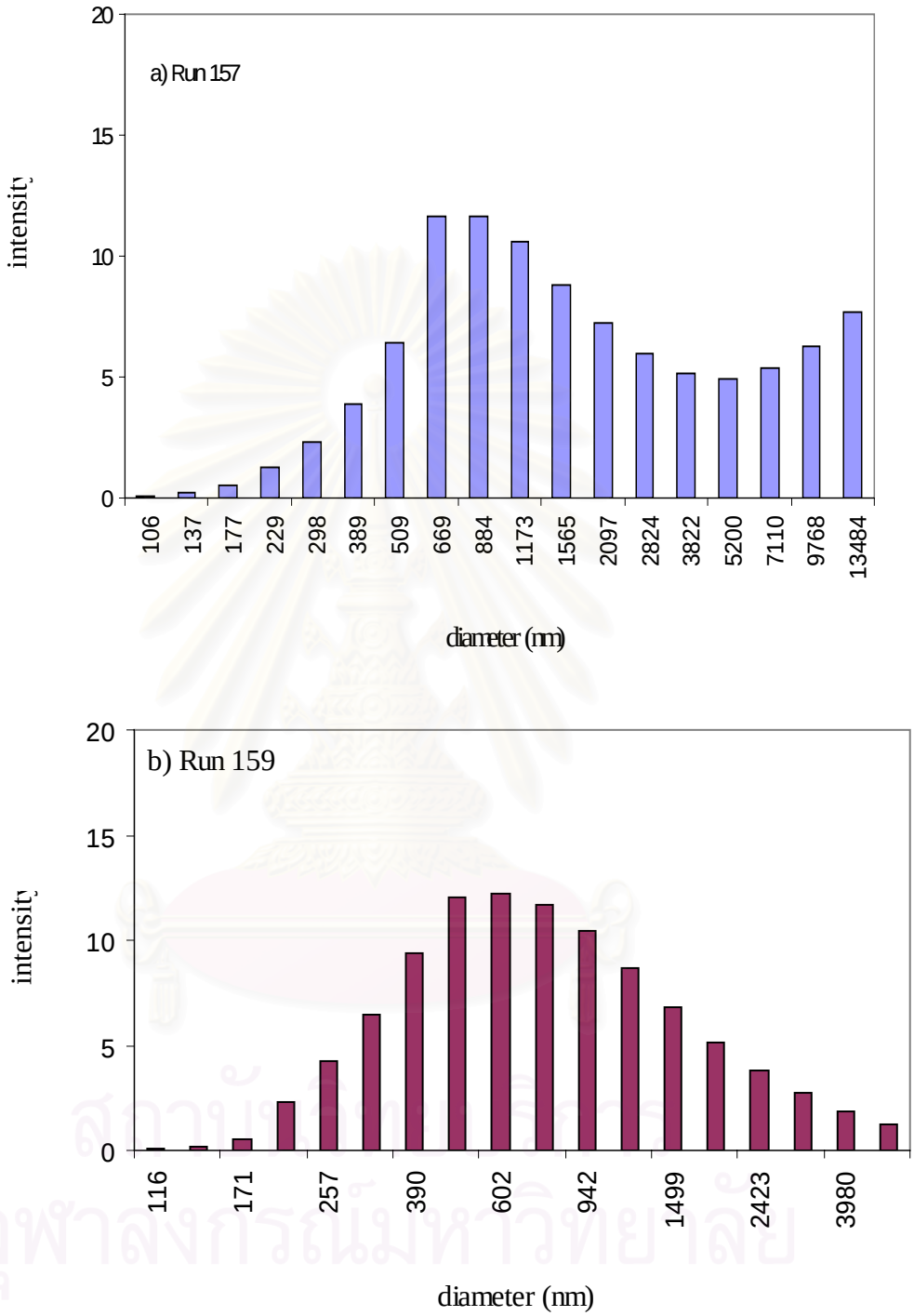

Figure 4.11 Histograms of the size distribution of the crosslinked P(DMAEMA-*co*-ST) particles using different crosslinking agents: (a) DVB (Run 157); (b) EGDMA (Run 159)

be consumed earlier. The reaction of EGDMA formed nuclei of the crosslinked copolymer. When the monomer mixture contains a crosslinking agent, the crosslinked copolymer becomes insoluble, both in the monomer and continuous phase [45]. Phase separation occurs between the ST and DMAEMA-rich phase, which yields coagulum. As mentioned above, this shows that the addition of a crosslinking agent has a favorable influence on the coagulum, which does not depend on the crosslinking agent type. Therefore, in order to investigate the effect of crosslinking agent types on the particle size, the latices were filtered to eliminate the coagulum. Then, the particle size of the crosslinked P(DMAEMA-*co*-ST) was observed by light scattering. Particle size histograms for the P(DMAEMA-*co*-ST) from different types of crosslinking agents are given in Figure 4.11, and show that the particle size increased when the crosslinking agent (DVB or EGDMA) was charged into the polymerization system. Furthermore, it seemed to depend on the type of crosslinking agent. In the presence of 10 wt% DVB, based on the monomer and crosslinking agent, the peak diameters of P(DMAEMA-*co*-ST) particles, with a bimodal size distribution, were located at 800 and 13484 nm as shown in Figure 4.11(a). In contrast, when adding 5 wt% EGDMA based on the monomer and crosslinking agent, the particle size was also smaller, as shown in Figure 4.11(b), and the mean particle diameter was around 602 nm. This result implies that the crosslinking agent only affects one monomer of the particle, i.e., DMAEMA or ST, rather than the whole particle because of the phase separation. This is because DVB is more hydrophobic than EGDMA.

4.1.3.4 Effect of V-50 Concentration

It is well known that the rate of initiation (R_i) is a function of the initiator efficiency (f), the initiator decomposition constant (k_d) and the initiator concentration ([I]), which can be expressed by the following equation (4.1):

$$R_i = 2 f k_d [I]. \quad (4.1)$$

The initiation is a two-step process. In the first step, the initiating radicals are formed by the decomposition of the initiator in the aqueous phase. Then, the hydrophilic primary radicals grow by propagation with a dissolved monomer in the aqueous phase to surface active oligomeric radicals. In the second step, the oligomeric radicals enter the monomer-swollen emulsifier micelles. The formed oligomer radicals enter the micelles and start the growth events [46].

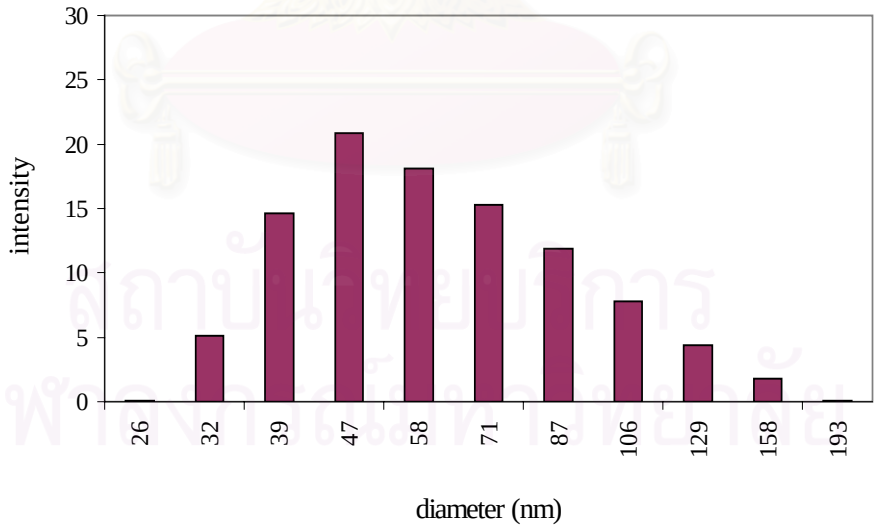

Figure 4.12 Histogram of the size distribution of the uncrosslinked P(DMAEMA-co-ST) particles using 5.0 wt% of V-50 (Run 160)

For this study, we studied uncrosslinked P(DMAEMA-*co*-ST) latex prepared by charging 2.0 and 5.0 wt% of V-50 (based on the monomer) in the emulsion polymerization of DMAEMA-ST co-monomers stabilized by CTAC (1.30 wt%) in Runs 154 and 160, respectively. Histograms of size distributions in Figure 4.10(b) and Figure 4.12 reveal similar profiles of polymer particles of DMAEMA-ST co-monomers. This shows that the mean particle size decreased from 117 to 47 nm as the concentration of V-50 increased from 2.0 to 5.0 wt%. The size distribution imposed by V-50 at a concentration of 5.0 wt% is rather narrow (CV = 18%). Two attributes are responsible for this result. First, the increasing formation of nuclei increased the number of radicals per particle. Simultaneous generation of single radicals in the particles promotes the narrow size distribution. Second, the increasing polymerization rate with greater initiator concentration is a consequence of the increasing flux of free radicals, which increases the probability of radical capture by droplets or by a monomer in the aqueous phase to induce formation of oligomers to produce active particles.

4.2 Preparation of PMMA Shells by Seeded Emulsion Polymerization

The preparation of PMMA shells using seeded emulsion polymerization was studied by two methods: swelling method and drop-by-drop method.

4.2.1 Swelling Method

The polymerization condition of the P(DMAEMA-*co*-ST) seed particles prepared by suspension polymerization is the same with that of Run 129 as shown in Table 4.2. The mean particle size was 1.52 μm (%CV = 30). Subsequently, P(DMAEMA-*co*-ST)/PMMA composite particle latices (Run 202) were prepared by

(DMAEMA-*co*-ST)-seeded emulsion polymerization of MMA employing swelling method using AIBN as an initiator. The appropriate condition is as follows:

Composition

P(DMAEMA-*co*-ST) (g)	100
$NaNO_2$ (g)	0.03
MMA (g)	10
AIBN (g)	0.2
Agitation rate (rpm)	100
Swelling time (h)	1
Polymerization temperature (K)	343
Polymerization time (h)	6

The TEM photograph of P(DMAEMA-*co*-ST)/PMMA composite particles (Run 202) with a batch monomer feed mode is shown in Figure 4.13. It was evident that the P(DMAEMA-*co*-ST)-pollen-like core was likely to be surrounded by the PMMA-petal-like shell or the PMMA core was to be sandwich-like with the P (DMAEMA-*co*-ST)-rich phase and agglomeration was occurred. From TEM photograph, we cannot conclude the optimum morphology for this method.

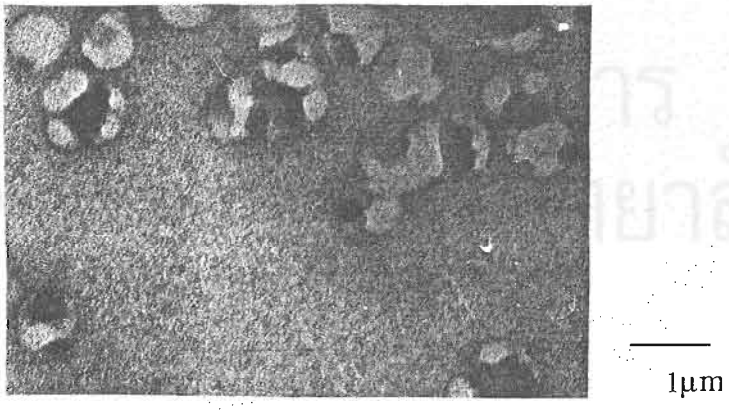

Figure 4.13 TEM photograph of P(DMAEMA-*co*-ST)/PMMA composite particles (Run 202) prepared by swelling method. [P(DMAEMA-*co*-ST) domain was stained with RuO_4].

4.2.2 Drop-by-Drop Method

The P(DMAEMA-*co*-ST) seed latices were employed without any post-treatment. The TEM photographs of P(DMAEMA-*co*-ST)/PMMA composite particles are shown in Figures 4.14 and 4.16 (see p. 75), where P(DMAEMA-*co*-ST)-rich domain was stained with RuO_4. As seen from TEM photographs, it is clear that the outer region of the composite particle is darker. This implies that the outer region of the composite particles corresponds to P(DMAEMA-*co*-ST)-rich phase, and the inner part corresponds to the PMMA-rich polymer formed at the second stage.

To obtain various morphologies and search for a polymerization condition to obtain core-shell P(DMAEMA-*co*-ST)/PMMA composite particles, initiator type, particle size and crosslinking agent type of the seed were changed.

4.2.2.1 Effect of the Initiator Type

Two initiators, V-50 and $K_2S_2O_8$, were used for the study under the same conditions summarized in Table 4.5. As shown in Figure 4.14(a), the morphology of the particles obtained in Run 217, where V-50 was added, exhibited a PMMA halfmoon-like morphology surrounded by P(DMAEMA-*co*-ST) shell. Moreover, the electron micrographs indicate a higher P(DMAEMA-*co*-ST) concentration at the outer part of the particles. This indicates that P(DMAEMA-*co*-ST) seed particles are more hydrophilic than PMMA. The second-stage PMMA polymer, containing the NH chain end groups from the initiator, possessed a high PMMA/water interfacial tension than the seed P(DMAEMA-*co*-ST) polymer phase. Therefore, the PMMA-rich phase tends to move into the internal domain of the particle to form a halfmoon-like domain.

Table 4.5 Recipe of P(DMAEMA-*co*-ST)/PMMA particles by seeded emulsion polymerization

Run No.	**217**	**218**	**221**	**222**	**223**
(Run of seed)	(153)	(154)	(157)	(159)	(160)
MMA (g)	10.00	10.00	10.00	10.00	10.00
V-50 (g)	0.20	-	0.20	0.20	0.20
$K_2S_2O_8$ (g)	-	0.20	-	-	-
Water (g)	10.01	10.06	20.56	20.25	20.11
Conversion	**78**	**82**	**89**	**79**	**80**
pH	8.56	9.13	8.40	8.24	8.61
ζ-potential (mv)	-	-88.0	-74.8	-85.2	-56.3
$\overline{M_n}^*$	4.22×10^4	4.97×10^4	7.78×10^4	9.01×10^4	2.70×10^4
$\overline{M_w}^*$	5.60×10^4	9.22×10^4	1.16×10^5	1.22×10^5	4.99×10^4
M_w/M_n	1.33	1.85	1.49	1.35	1.85
d_p (nm)	157	207	coagulum	coagulum	55
d_p of seed (nm)	129	117	coagulum	coagulum	47
%CV	21	25	-	-	20

Agitation rate 120 rpm, bubbling N_2 for1 h, polymerization temp. 374 K, adding initiator immediately, adding MMA 0.17 cm^3 min^{-1}, polymerization time of 6 h, *THF soluble fraction

The particles obtained in Run 218 had a different morphology from that prepared in Run 217 [Figure 4.14 (b)]. Although the PMMA particles from Run 218 were surrounded by a P(DMAEMA-*co*-ST) shell, the small P(DMAEMA-*co*-ST)-rich phase was also distributed inside of the PMMA core. This indicates that, under the same experimental conditions (Runs 217 and 218), the radicals derived from KPS,

when captured by the particles, had a higher mobility in the P(DMAEMA-*co*-ST) phase swollen by the PMMA phase than those from V-50. The difference in the observed core structures indicated that oligomeric radicals containing sulfate end-groups could penetrate more deeply into the P(DMAEMA-*co*-ST) seed particle surface than could the radicals derived from V-50. The second-stage PMMA polymer with SO_4^- chain end groups from initiator exhibited a low PMMA/water interface than P(DMAEMA-*co*-ST) seed particles.

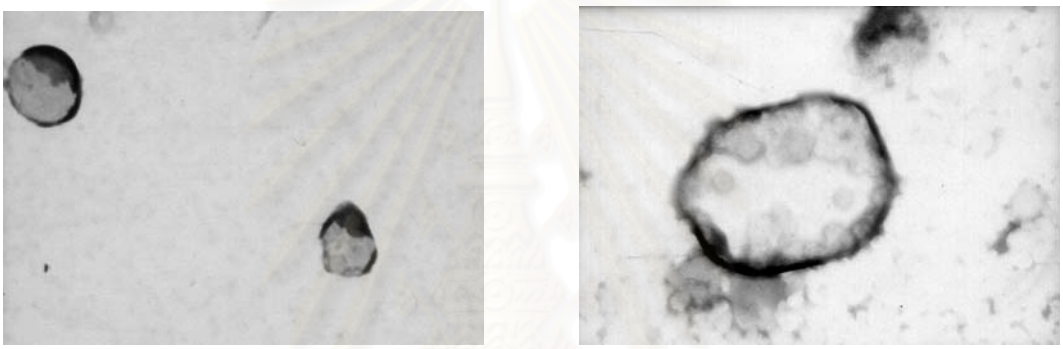

(a) (b)

Figure 4.14 TEM photographs of P(DMAEMA-*co*-ST)/PMMA composite particles using various initiator types; (a) Seed: Run 153 with V-50 (Run217), (b) Seed: Run 154 with KPS (Run 218). [P(DMAEMA-*co*-ST) domain was stained with RuO_4].

Jonsson [26] reported that the type of second-stage initiator had a strong effect on the morphology of the composite particles prepared even under monomer-starved conditions. The particle surface polarity is determined by the functional groups, which result from the initiator fragments. These surface polarities of latex particles are key parameters in deciding which phase is inside or outside in composite particles. In this hypothesis, the surface-active oligomeric radicals formed in the aqueous phase by the decomposition of the water-soluble initiator (potassium

persulfate) and the addition of monomer molecules, adsorbed onto the particle surface and become incorporated in the particles by continuing adding the new monomer molecules. The monomer molecules can diffuse slowly under the same conditions. Therefore, the newly-formed polymer chains are likely to remain closer to the particle surface. Due to their polar initiator groups (sulfate), the previously formed polymer chains remained anchored to the sulfated particles with one chain end, even when they are forced away from the interface into the interior of the particle by new growing chains. The strain then becomes too great for the polymer molecules formed early in the reaction, and the sulfate end-groups are pulled away from the surface into the interior of the particle. This is because the polymer chains with V-50 fragments show lower polarity than those with KPS fragments, hence leading to higher interfacial tension between the polymer and the aqueous phase and between the two polymers.

4.2.2.2 Effect of Particle Size of P(DMAEMA-*co*-ST) Seed

The seed latex of Run 160 was used, which was prepared by charging 5.0 wt% of V-50 in the emulsion polymerization. As shown in Table 4.4, the mean particle size of seed latex was 47 nm. P(DMAEMA-*co*-ST)/PMMA composite particles prepared with V-50 and KPS as initiators in Runs 217 and 218, respectively, exhibited a dense shell layer with a rather well defined interface between PMMA and P(DMAEMA-*co*-ST). As shown in Figure 4.15, P(DMAEMA-*co*-ST)/PMMA composite particles (Run 223), in which V-50 was used as an initiator, formed a cloudy shell layer and seemed to be diluted with PMMA domains. In this case the shell layer was thinner and more irregular in shape than that in Run 217 and 218. Similar differences in shell-layer morphology were produced by substituting KPS for V-50. Run 223 was performed under conditions similar to those of Run 217,

except for the fact that the smaller seed particles contained higher V-50 radical fragments.

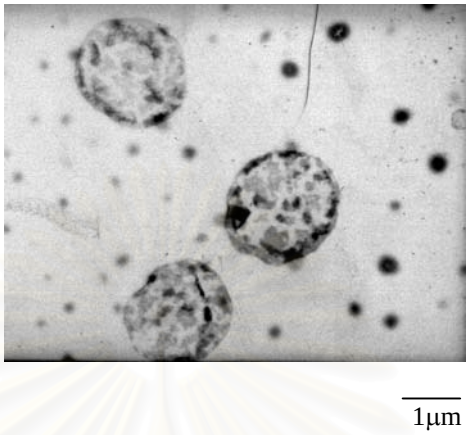

Figure 4.15 TEM photograph of P(DMAEMA-*co*-ST)/PMMA composite particles using small particle sized seed (Run 160). [P(DMAEMA-*co*-ST) domain was stained with RuO_4].

According to the Fitch-Tsai theory of emulsion polymerization, if the number of primary particles is high enough, the new particles will not form. However, in the present case, it seemed impossible to drastically increase the number of seed particles without changing other properties of the seed particles [47]. For example, when using the seed latex (Run 160), the changes of the particle size affected the morphology of resultant particles. Figure 4.15 shows the results of using the P(DMAEMA-*co*-ST) seed latices of Run 160 while maintaining the same condition of seeded emulsion polymerization. The small P(DMAEMA-*co*-ST)-rich phase was distributed inside of the PMMA-rich phase surrounded by P(DMAEMA-*co*-ST) shell. In this seeded emulsion polymerization, it is clearly shown in Figure 4.15 that the morphology was much affected by the particle size of seed latex.

4.2.2.3 Effect of Crosslinking Agent Type of P(DMAEMA-*co*-ST) Seed

Generally, crosslinking of the seed particles would result in an enhancement of phase separation, and in most cases hemispherical or structures with multiple surface domains would be obtained. By crosslinking at least one of the polymer phases, the chain mobility is limited.

The TEM micrographs using different crosslinked P(DMAEMA-*co*-ST) seed particles prepared under identical conditions are shown in Figure 4.16. It has been reported in the previous section that, the addition of 10 wt% of DVB, the seed latices were filtered to eliminate the coagulum prior to the seeded emulsion polymerization. Using these seed latices, as shown in Figure 4.16(a), invert core-shell P(DMAEMA-*co*-ST)/PMMA composite particles were obtained, even when changing the crosslinking agent type to 5 wt% of EGDMA as shown in Figure 4.16(b). This indicates that the miscibility of seed polymer and crosslinking agent, DVB or EGDMA, was too poor to prevent the solubility of DMAEMA from the seed particles and inhibit diffusion of the PMMA into the interior of the P(DMAEMA-*co*-ST) seed particles. As a consequence, we found that PMMA migrates into the crosslinked P(DMAEMA-*co*-ST), and polymerized there. The PMMA–rich phase was halfmoon-like, laying inside of the P(DMAEMA-*co*-ST)-rich phase as shown in Figure 4.16.

As a result, it was found that crosslinked P(DMAEMA-*co*-ST) seed latex with EGDMA or DVB was not effective for localization of P(DMAEMA-*co*-ST) domains in the resultant particle, and they are thus not essential for the preparation of P(DMAEMA-*co*-ST) seed particles. Possibly, filtered-out coagulums may have incorporated DVB or EGDMA preferentially. Comparing Figures 4.16(a) and (b), it is evident that the morphology of P(DMAEMA-*co*-ST)/PMMA composite

particles in Run 222 is similar with that in Run 221. This is because the crosslinking agent (DVB or EGDMA) affects significantly the coagulum formation of PDMAEMA copolymers in the emulsion polymerizations.

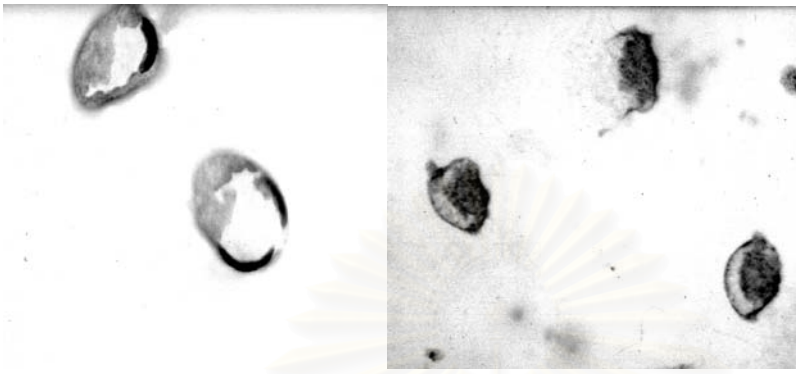

(a) Run 221 1μm (b) Run 222 1μm

Figure 4.16 TEM photographs of P(DMAEMA-*co*-ST)/PMMA composite particles using various types of crosslinking agent of P(DMAEMA-*co*-ST) seed; (a) Seed: Run 158. DVB: 10 %w/w (Run 221), (b) Seed: Run 159. EGDMA: 5%w/w (Run 222). [P(DMAEMA-*co*-ST) domain was stained with RuO_4].

4.3 Preparation of PST Outer Shells by Seeded Emulsion Polymerization

4.3.1 Heterocoagulation

In the stepwise heterocoagulation carried out at the cationic PST-to-anionic P(DMAEMA-*co*-ST) ratio of about 33:67 (w/w), the condition for such a synthesis of polymer was studied by varying the SDS concentration.

4.3.1.1 Cationic PST Emulsion

Cationic PST particles were produced by emulsion polymerization, which appropriate condition is as follows:

Composition		**Result**	
Water (g)	200	Conversion	90
CTAC (g)	2.5	d_p (μm)	0.11
ST (g)	67.005	%CV	11.16
V-50 (g)	0.250	pH	9.01
Water (g)	20.027	ζ-potential (mV)	+94
Total wt. (g)	289.782		

Agitation rate 160 rpm, bubbling N_2 for 1 h, polymerization temperature 333 K, adding V-50 immediately, polymerization time of 4h.

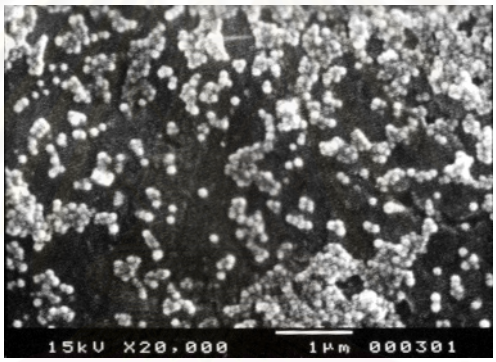

Figure 4.17 SEM photograph of cationic PST particles (Run 301)

The resulting properties of the PST latex are shown above in the right column. As shown in Figure 4.17 for the SEM photograph of the PST particles (Run 301), the mean diameter is 0.11 μm and the coefficient of variation is 11.16%. Corresponding to the use of cationic V-50 and CTAC, ζ-potential revealed a fairly positive value.

4.3.1.2 Anionic P(DMAEMA-*co*-ST)/PMMA Particles

The polymerization results of the P(DMAEMA-*co*-ST) seed particles prepared by suspension polymerization using AIBN as an initiator (Run 129) have

already shown in Table 4.2, and the SEM photographs of the seed particles have already shown in Figure 4.6. The mean particle size was approximately 1.29 μm (%CV = 30) and they were used as anionic P(DMAEMA-*co*-ST) particles (pH = 9.14, ζ-potential = -40.2). Subsequently, P(DMAEMA-*co*-ST)/PMMA composite particles were synthesized by seeded emulsion polymerization, using the above latex (Run 129) as a seed and MMA as the monomer with V-50 as an initiator. It was found that the pH of the reaction mixture was 8.63 and the ζ-potential of the latex particles gave a negative value. As shown in the TEM photograph of Figure 4.16, the mean particle size of P(DMAEMA-*co*-ST)/PMMA particles was 1.68 μm. It is evident that the PMMA-rich core is likely to be surrounded by P(DMAEMA-*co*-ST)-rich shell, because the hydrophilicity of P(DMAEMA-*co*-ST) is higher than that of PMMA.

4.3.1.3 Blend Emulsion by the Stepwise Heterocoagulation Method

Table 4.6 shows the recipes of blend emulsion by the stepwise heterocoagulation method. In Table 4.6, two sets of emulsion was prepared.

4.3.1.3.1 Effect of SDS Concentration

As seen from Table 4.6 and Figure 4.18, the SDS concentration affected the colloid stability of the heterocoagulated emulsion in the resultant particles. Comparing Runs 403 and 404, where the P(DMAEMA-*co*-ST)/PMMA-to-PST ratio was about 67/33 (%w/%w), it was found that the some heterocoagulated particles were formed as shown in Figure 4.18 after being gently stirred for 1 h. Furthermore, it was observed that the stable heterocoagulated composite emulsion prepared by adding SDS (Run 403) in the anionic P(DMAEMA-*co*-ST)/PMMA latex is better. However, the heterocoagulation between

P(DMAEMA-*co*-ST)/PMMA and PST was not complete. Therefore, the seeded emulsion polymerization method was employed in the following experiments.

Table 4.6 Recipes of heterocoagulation for the preparations of cationic small PST particles and anionic large P(DMAEMA-*co*-ST) particles

Run No.	**403**	**404**
P(DMAEMA-*co*-ST)/PMMA (g)	20	20
SDS (g)	0.1	-
KCl (g)	0.01	0.01
IPA (g)	0.5	0.5
PST (g)	10	10
Water (g)	29	29
IPA (g)	1.0	1.0
KCl (g)	0.02	0.02
ζ-potential (mV)	-28	-30

Agitation rate 160 rpm, flow rate of PST 0.67 cm^3 min^{-1}, mixing temperature 333 K, and mixing time 1 h

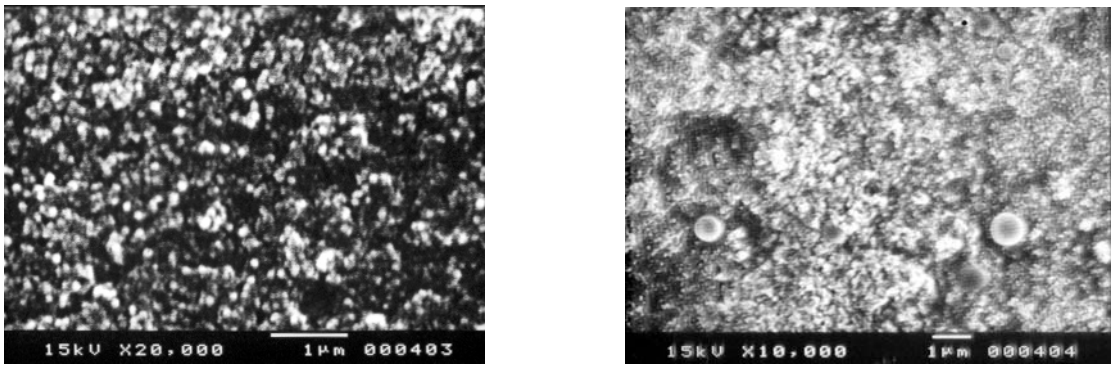

(a) (b)

Figure 4.18 SEM photographs of the P(DMAEMA-*co*-ST)/PMMA/PST particles prepared by heterocoagulation at various concentrations of SDS: (a) 0.1 g (Run 403); (b) without SDS (Run 404).

4.3.2 Seeded Emulsion Polymerization of P(DMAEMA-*co*-ST)/PMMA/PST Composite Particles

Five P(DMAEMA-*co*-ST)/PMMA latex samples, which differ in their particle surface polarity were characterized as seed latices. The ζ-potential of the final latex particles remained negative, although the absolute value became smaller. Seeded emulsion polymerization seemed to take place in the second and final stage when a part of the negative surface charge was neutralized with the counter ions, and the particle size became bigger. The P(DMAEMA-*co*-ST)/PMMA/PST composite polymer formulations are shown in Table 4.7.

Table 4.7 Recipe of P(DMAEMA-co-ST)/PMMA/PS composite particles by seeded emulsion polymerization

Run No.	**409**	**410**	**412**	**413**	**414**
(Run of seed)	(217)	(218)	(221)	(222)	(223)
ST (g)	**10.00**	**10.00**	**10.00**	**10.00**	**10.00**
V-50 (g)	0.20	0.20	0.20	0.20	0.20
Water (g)	10.05	10.01	20.55	20.07	20.14
Conversion	93	90	95	89	92
pH	8.93	8.89	8.93	7.80	8.29
ζ-potential (mv)	-98.0	-64.5	-60.8	-86.0	-51.3
$\overline{M_n}^*$	9.99×10^4	1.21×10^5	7.43×10^4	3.42×10^4	5.71×10^4
$\overline{M_w}^*$	2.93×10^5	2.85×10^5	1.49×10^6	2.02×10^5	2.05×10^5
M_w/M_n	2.94	2.37	20.05	5.90	3.59
d_p (nm)	163	351	coagulum	coagulum	61
%CV	30	29	-	-	25

Agitation rate 120 rpm, bubbling N_2 1h, temp. 374 K, adding V-50 immediately, adding ST 0.17 $cm^3\,min^{-1}$, polymerization time 8 h, * THF soluble fraction

4.3.2.1 Morphology of the P(DMAEMA-*co*-ST)/PMMA/PST Composite Particles

Figure 4.19 shows that all P(DMAEMA-*co*-ST)/PMMA seed latices were equally well covered with PST shell (Runs 409, 410, 412 and 413), regardless of their molecular weight differences. Except for Run 414, the particles consisted of a PMMA shell layer surrounding an inverted core-shell [PST-core, P(DMAEMA-*co*-ST)-shell] as shown in Figure 4.19(e).

The morphology of the particles obtained in Run 409 using the seed from Run 217, exhibited a PMMA-halfmoon-like/P(DMAEMA-*co*-ST) composite particles surrounded by PST-rich shell and the secondary particles were observed in Figure 4.19(a). The P(DMAEMA-*co*-ST)/PMMA/PST composite particles of Run 410 using

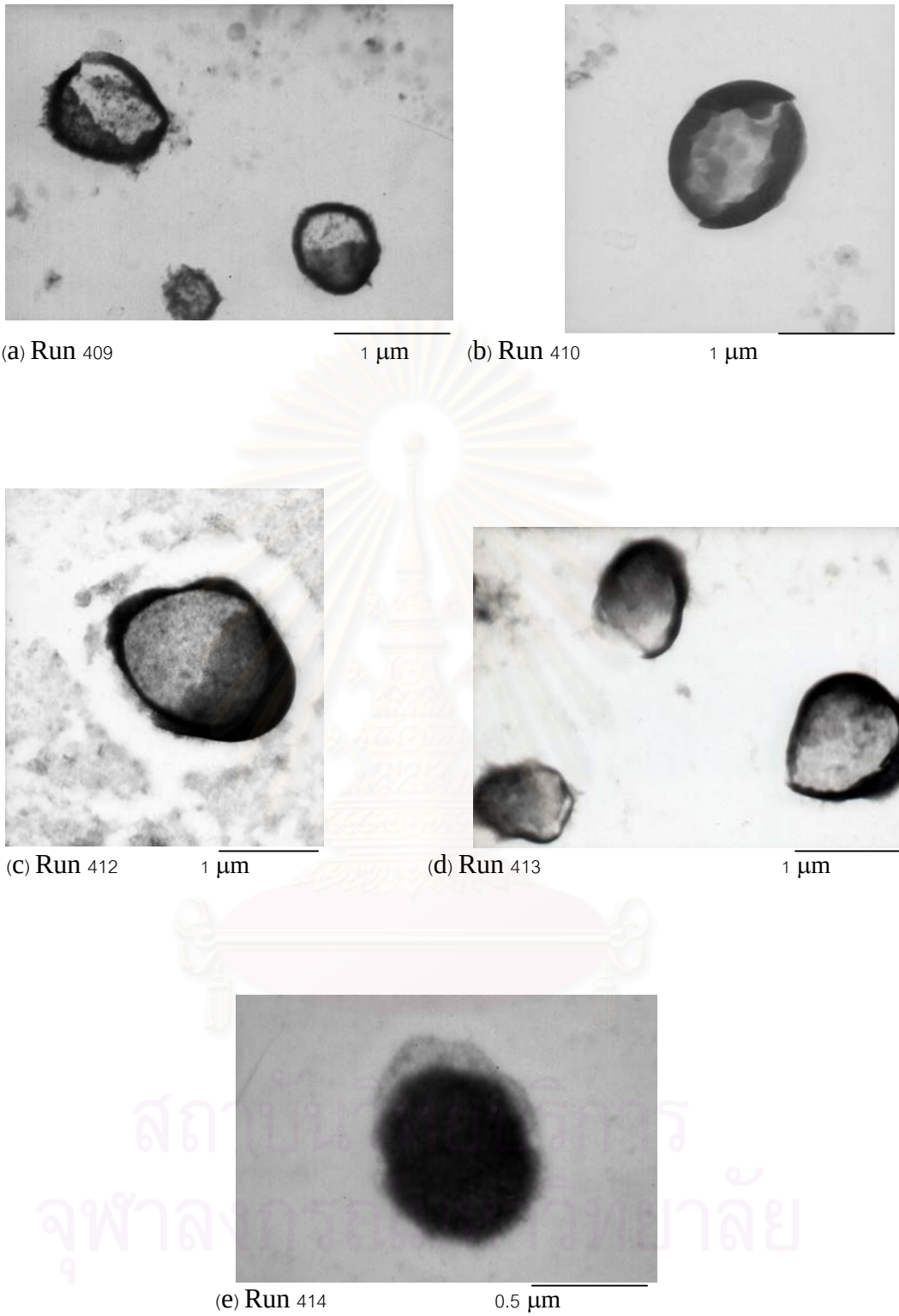

Figure 4.19 TEM photographs of P(DMAEMA-*co*-ST)/PMMA/PST composite particles from seed particles having different morphologies; (a) Seed: Run 217, (b) Seed: Run 218, (c) Seed: Run 221, (d) Seed: Run 222, (e) Seed: Run 223. [P(DMAEMA-*co*-ST) and PST domains were stained with RuO_4].

the seed from Run 218 were prepared under conditions similar to those of Run 409, except for the fact that the seed particles contained a hydrophilic initiator, KPS. The particles obtained from Run 410 as shown in Figure 4.19(b) consisted of a PST shell layer surrounding a PMMA core containing small P(DMAEMA-*co*-ST) domains.

The P(DMAEMA-*co*-ST)/PMMA/PST composite particles obtained in Runs 412, and 413 [Figure 4.19(c) and (d)] under the same condition using the different crosslinked seeds in Runs 222 and 223, respectively, had the morphology similar to those of Run 409. However, the formation of coagulum in the final stage polymerization in Run 412 from which crosslinked P(DMAEMA-*co*-ST) particles with 10%wt DVB were used indicates the greater extent of phase separation. The same tendency has been found in the crosslinked P(DMAEMA-*co*-ST) seed with 5%wt EGDMA system as shown in Figure 4.20. This result implies that the type of crosslinking agent for P(DMAEMA-*co*-ST) seeds does not influence the morphology of P(DMAEMA-*co*-ST)/PMMA composite particles. This is because the crosslinking agent (DVB or EGDMA) contributed to the coagulum formation of PDMAEMA copolymers significantly in the emulsion polymerizations. It was found that the coagulum of the latex was observed when using crosslinked P(DMAEMA-*co*-ST) seeds for polymerization. The SEM photographs showing the effect of crosslinking agent on the coagulum in both Runs 221 and 222 are shown in Figure 4.20.

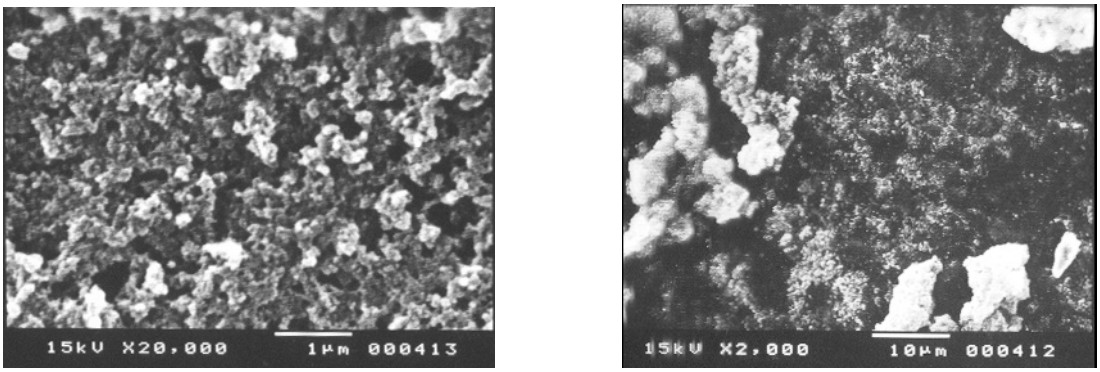

(a) Run 412 (b) Run 413

Figure 4.20 SEM photographs of P(DMAEMA-*co*-ST)/PMMA/PST composite particles using various types of crosslinking agent for P(DMAEMA-*co*-ST) seeds; (a) Seed: Run 158. DVB: 10 %w/w (Run 412), (b) Seed: Run 159. EGDMA: 5%w/w (Run 413).

The morphology of the P(DMAEMA-*co*-ST)/PMMA/PST composite latex using the P(DMAEMA-*co*-ST)/PMMA seeds in Run 223, where the averaged molecular weight of seeds is low (see Table 4.5), is shown in Figure 4.19(e). The TEM photograph [Figure 4.19(e)] shows that the final stage polymer PST-rich phase [(the darker region) partially engulfed by P(DMAEMA-*co*-ST)-rich phase (gray region)], covered the PMMA-rich phase (lighter region) in Run 414. In agreement with Lee et al. [28], the inverted core-shell morphology is favored by lower molecular weight of hydrophilic seed polymer. The higher the hydrophilicity, the greater the phase separation was found between polymers I and II.

From the above results, it can be concluded that a different core-shell composite particle could be prepared by seeded emulsion polymerization. It is important to know that halfmoon-like morphology can be obtained using V-50 even for the P(DMAEMA-*co*-ST)/PMMA system. For this system, a PMMA-core/P(DMAEMA-*co*-ST) shell morphology is usually formed, because the

hydrophilicity of P(DMAEMA-*co*-ST) is higher than that of PMMA. From the above results in the final stage, it is apparent that the composite microspheres were always surrounded by a PST-rich shell, when V-50 is used as an initiator. This is because V-50 is hydrophilic and the interfacial tension between PST-rich polymer with the V-50 fragment and the water is lower. However, multi-layered composite microspheres were not obtained, even by changing the initiator from V-50 to KPS. This is probably because the hydrophilicity of PDMAEMA is much higher than that of PMMA. It is postulated that the multi-layered P(DMAEMA-*co*-ST)/PMMA/PST composite microsphere structure is more favored than the halfmoon-like microsphere structure for applications of outdoor coating, such as, a UV-radiation scattering additive in paints.

4.4 Properties of Composite Polymers

P(DMAEMA-*co*-ST)/PMMA and P(DMAEMA-*co*-ST)/PMMA/PST composite polymers were prepared by seeded emulsion polymerization. The composite polymer formulations are showed in Tables 4.5 and 4.7. The properties of the composite polymers were measured and the results obtained are presented as follows:

4.4.1 Average Molecular Weight of PMMA and PST Shells

The average molecular weights of THF soluble fractions which are PMMA and PST are shown in Tables 4.8 and 4.9. The average molecular weights ($\overline{M_w}$) of PMMA shells (Runs 217, 218, 221, 222, and 223) were roughly from 4.99 x 10^4 to 1.22 x 10^5. This result indicates that the average molecular weights of PMMA shells were low. This is because some PMMA and P(DMAEMA-*co*-ST) were sacrificed as homopolymer or copolymer. For P(DMAEMA-*co*-ST)/PMMA/PST composite

polymers (Runs 409, 410, 412, 413, and 414), the average molecular weights of PMMA and PST shells were roughly from 2.02 x 10^5 to 1.49 x 10^6. The effect of the crosslinking agent (DVB or EGDMA) of P(DMAEMA-co-ST) seeds on the molecular weights of shells is shown in Runs 221, 222, 412, and 413. We found that the average molecular weights of polymer shells were insignificant different from those of shells of uncrosslinked composite polymers because the addition of the crosslinking agent had a favorable influence on the coagulum formation as mentioned above.

Table 4.8 Characterization of P(DMAEMA-*co*-ST)/PMMA composite polymers

Run No.	$\overline{M_n}$	$\overline{M_w}$	$\mathbf{M_w/M_n}$
217	4.22×10^4	5.60×10^4	1.33
218	4.97×10^4	9.22×10^4	1.85
221	7.78×10^4	1.16×10^5	1.49
222	9.01×10^4	1.22×10^5	1.35
223	2.70×10^4	4.99×10^4	1.85

Table 4.9 Characterization of P(DMAEMA-*co*-ST)/PMMA/PST composite polymers

Run No.	$\overline{M_n}$	$\overline{M_w}$	M_w/M_n
409	9.99×10^4	2.93×10^5	2.94
410	1.21×10^5	2.85×10^5	2.37
412	7.43×10^4	1.49×10^6	20.05
413	3.42×10^4	2.02×10^5	5.90
414	5.71×10^4	2.05×10^5	3.59

4.4.2 Refractive Index of Composite Polymers

4.4.2.1 Latex Film Preparation

Films of P(DMAEMA-*co*-ST) latex (Tables 4.2 and 4.4), prepared by suspension and emulsion polymerization, and P(DMAEMA-*co*-ST)/PMMA composite latex samples (Table 4.5), prepared by seeded emulsion polymerization, were dried at room temperature. All of them formed transparent films even though their preparation methods and particle structure were different. This is because PDMAEMA and PMMA are transparent. On the other hand, the difference in particle structure of P(DMAEMA-*co*-ST)/PMMA/PST composite latex was illustrated by the state of film formation. Since P(DMAEMA-*co*-ST)/PMMA/PST composite latex using KPS as an initiator (Run 410) formed an opaque, white film, whereas P(DMAEMA-*co*-ST)/PMMA/PST composite latex using V-50 as an initiator (Run 409 and 414) formed a transparent film. This difference in film morphology is attributed to the variation in morphology and refractive index of the P(DMAEMA-*co*-ST)/PMMA/PST composite latex particles. It has been understood that if a medium is transparent, the unreflected light will be transmitted, some of the transmitted light will be absorbed as heat, some will be transmitted, and some will be reflected, often at selected wavelengths, imparting color to the medium. If the medium is opaque, this process takes place entirely and immediately within the surface, with no light being transmitted.

4.4.2.2 Evaluation of Refractive Index of Film

Three P(DMAEMA-*co*-ST)/PMMA/PST latex films of Runs 409, 410, and 414, which differ in their particle size and morphology were prepared by spin

coating the latex on a silica plate for refractive index measurements. The other samples were not enough to prepare film samples, so we cannot compare the reflective index of the polymer shell.

The results of the measurements, as shown in Table 4.10, comprise a list of the observed modes of the film, identified by their mode numbers m = 0 and 1. For simplicity, we assumed that all modes have the same polarization. The observed propagation constants, N_0 and N_1, are related to the unknowns n and W by the dispersion equation of the planar dielectric guide. The equations concerned are the following:

$$N_m = \sin\alpha \cos\varepsilon + (n_p^2 - \sin^2\alpha)^{1/2} \sin\varepsilon, \quad (4.2)$$

$$\mathbf{kW(n^2 - N_m^2)^{1/2} = \Psi_m (n, N_m),} \quad \mathbf{(4.3)}$$

$$\Psi_m (n, N_m) \equiv m\pi + \phi_0(n, N_m) + \phi_2(n, N_m), \quad (4.4)$$

and

$$\phi_j(n, N_m) \equiv \arctan[(n/n_j)^{2\rho} (N_m^2 - n_j^2/n^2 - N_m^2)]^{1/2}, \quad (4.5)$$

with j = 0 (air), 2 (substrate), where N_m is the propagation constant, α is the incident angle to the prism, ε is the angle of the prism ($\varepsilon = 40^o$), k is the wave number of the incident laser beam in vacuum, m is the mode number, n_p and n are the refractive indices of the prism (n_p = 1.92588), and films, and W is the thickness of films. Inserting N_0 and N_1 into Eqs. (4.3) to (4.5), one yields two equations from which kW can be eliminated. Refractive index (n) was calculated by the least-squares fitting (LSF) method with the appropriate values for n_p, ε, and α.

Table 4.10 Refractive Index of P(DMAEMA-*co*-ST)/PMMA/PST composite polymers

Run No. (Initiator Type)	Incident Angle (α)	Film Formation	Refractive Index (n)	Reflection (%)
409 (V-50)	25	transparent	1.606	5.41
410 (KPS)	42	opaque, white	1.755	7.51
414 (V-50)	19	transparent	1.541	4.53

Table 4.10 reveals the film refractive index of P(DMAEMA-*co*-ST)/PMMA/PST composite polymers. The results show that the reflection and refractive index of the PST shell layer surrounding the PMMA core containing the small P(DMAEMA-*co*-ST) domains (Run 410) is higher than that of the PMMA halfmoon-like/P(DMAEMA-*co*-ST) composite particles surrounded by the PST-rich shell (Run 409) and the PST-rich phase partially engulfed by the P(DMAEMA-*co*-ST)-rich phase as a core covered by the PMMA-rich shell (Run 414). This is because the refractive index of PST is higher than that of the PMMA and P(DMAEMA-*co*-ST) and particle size of Run 414 is smaller than that of Run 409 and 410. It has been a common knowledge that when a light beam passes from a medium of higher refractive index to one of lower refractive index, the angle of the beam increased. If the angle of incidence is high enough, all light is reflected back and none is transmitted out. In almost all coatings, the smaller the particle size, the greater the absorption. From above results, it can be concluded that the refractive index depended on the morphology and particle size of P(DMAEMA-*co*-ST)/PMMA/PST composite polymers.

CHAPTER V

CONCLUSIONS AND SUGGESTIONS

5.1 Conclusions

In this research, several reaction parameters affecting the properties and morphology of the composite polymers were investigated. The results can be summarized as the following.

5.1.1 Preparation of PDMAEMA Core Particles

The polymerization of hydrophilic monomer DMAEMA is highly sensitive to the nature of the initiators such as AIBN, KPS, and V-50. The addition of AIBN to the suspension polymerization system containing PEO23, water and EA at 343 K led to the particle diameter in range of micrometers and a broad size distribution. In the contrary, emulsion polymerization of DMAEMA initiated by V-50 at 343 K using CTAC as a stabilizer led to small particle diameters of approximately 117 nm and a narrow size distribution. The stable P(DMAEMA-*co*-ST) latices were formed as well as the final conversion was higher than 60%. However, it was found that MMA as a co-monomer influenced the morphology and stability of the PDMAEMA particles formed. When the PDMAEMA contained 20 wt% of MMA, the P(DMAEMA-*co*-MMA) particles were deformed, sticky, and unstable. Addition of crosslinking agent, EGDMA or DVB, led to the coagulum formation of PDMAEMA copolymer particles in both of the suspension polymerization and emulsion polymerization due to phase separation.

5.1.2 Preparation of PMMA Shells and PST Shells

P(DMAEMA-*co*-ST)/PMMA/PST composite particle latices were prepared by P(DMAEMA-*co*-ST)-seeded emulsion polymerization of MMA as a second-stage monomer and ST as a final-stage monomer, respectively, employing a stepwise addition method. P(DMAEMA-*co*-ST)/PMMA composite latices were synthesized by polymerizing MMA in the presence of P(DMAEMA-*co*-ST) seed particles. The effects of the type of initiators (V-50 or KPS), the particle size, and crosslinking agent types of the seed latices on the morphology of P(DMAEMA-*co*-ST)/PMMA composite particles were investigated. It was found that the particle morphology was an invert hemicore-shell surrounded by a P(DMAEMA-*co*-ST)-rich shell when V-50 was used as an initiator, while the small P(DMAEMA-*co*-ST)-rich phase was distributed inside of the PMMA-rich phase surrounded by P(DMAEMA-*co*-ST) shell. These results proved that the initiator type is one of the main parameters controlling particle morphology in composite latices. Subsequently, P(DMAEMA-*co*-ST)/PMMA/PST composite particles were prepared by polymerizing ST, using the above latex as a seed polymer. It was found that P(DMAEMA-*co*-ST)/PMMA composite latices were engulfed by the PST-rich polymer when higher molecular weight of the hydrophilic P(DMAEMA-*co*-ST)/PMMA composite particles were used, while PST-rich phase partially engulfed by the P(DMAEMA-*co*-ST)-rich phase as a core covered by the PMMA-rich shell was obtained when the hydrophilic P(DMAEMA-*co*-ST)/PMMA composite particles having lower molecular weight were used. In this case, crosslinked P(DMAEMA-*co*-ST) seed particles did not affect the morphology of composite polymers. Furthermore, the coagulum formation occurred in all steps due to the addition of crosslinking agent in the first step. The

refractive index depended on the morphology and particle size of composite polymers.

5.2 Suggestions for Future Work

Synthesis of the composite particles with the morphology of P(DMAEMA-*co*-ST)/PMMA/PST should be further studied as follows:

1. The synthesized PDMAEMA copolymers used as a seed are not uniform, so it is difficult to synthesize and characterize PMMA and PST shells when this polymer is used in the proceeding steps. We recommend that the types of nonionic stabilizers, initiators, and co-monomer, be changed, since the optimum condition for uniform PDMAEMA seeds is indeed altered.
2. The crosslinking agent should be added to the second and third stage of polymerization in order to obtained the expected morphology.

REFERENCES

1. Nikaya, T.; Fukushima, Y.; Kikuta, T. Highly Weather-Resistant, Single Package, Crosslinkable Emulsion, *U.S. Pat. 5 534 579*, 1996.
2. Yu, Z-Q.; Li, B-G.; Li, B-F.; Pan, Z-R. Preparation and Characterization of MMA-BA-DMAEMA Terpolymer latex. *J Colloid Surf A: Physicochem. Eng. Aspects.* 153 (1999): 31-38.
3. Kawaguchi, H.; Fujimoto, K.; Saito, M.; Kawasaki, T.; Uragami, Y.; Mizuhara, Y. Monodisperse Hydrogel Microspheres: Their Features and Application. *In Preprints of the International Symposium on Polymeric Microspheres*, Oct. 23-29, 1991, 119. (Organized by Center for Cooperative Research in Science and Technology, Fukui University, Japan)
4. Cao, K.; Li, B.-G.; Pan, Z.-R. Micron-size Uniform Poly(methyl methacrylate) Particles by Dispersion Polymerization in Polar Media. IV. Monomer Partition and Locus of Polymerization. *J Colloid Surf A: Physicochem. Eng. Aspects*, 153 (1999): 179-187.
5. Sundberg, E. J.; Sundberg, D.C. Morphology Development for Three-Component Emulsion Polymers: Theory and Experiments. *J. Appl. Polym. Sci.*, 47 (1993): 1277-1294.
6. Ma, G.H. Advances in Preparations and Applications of Polymeric Microspheres. In K. Esumei (eds.), *Polymer Interfaces and Emulsions.* p. 77. New York: Marcel Dekker Inc., 1998.
7. Ma, G.H. Advances in Preparations and Applications of Polymeric Microspheres. In K. Esumei (eds.), *Polymer Interfaces and Emulsions.* p. 75. New York: Marcel Dekker Inc., 1998.

8. Omi, S.; Katami, K.; Yamamoto, A.; Iso, M. Synthesis of Polymeric Microspheres Employing SPG Emulsification Technique. *J. Appl. Polym. Sci.* 51(1994): 1-11.

9. Ma, G.H. Advances in Preparations and Applications of Polymeric Microspheres. In K. Esumei (eds.), *Polymer Interfaces and Emulsions.* p. 57. New York: Marcel Dekker Inc., 1998.

10. El-Aasser, M.S.; Sudol, E.D. Features of Emulsion Polymerization. In P.A. Lovell, and M.S. El-Aasser (eds.), *Emulsion Polymerization and Emulsion Polymers.* pp. 52-53. New York: John Wiley & Sons, 1997.

11. Akkarakittimongkol, P. *Comparision of the Synthesis of Acrylate Core/Shell.* Master's Thesis, Graduate School, Chulalongkorn University, 2000.

12. Segall, I.; Dimonie, V.L.; El-Aasser, M.S.; Soskey, P.R.; Mylonakis, S.G. Copolymerization of Styrene/Benzyl Methacrylate as Choice for Shell Material and Characterization of Poly(n-butyl acrylate) Core Latex Particles. *J. Appl. Polym. Sci.* 58(1995): 385-399.

13. Ottewill, R.H. Stabilization of Polymer Colloid Dispersions. In P.A. Lovell, and M.S. El-Aasser (eds.), *Emulsion Polymerization and Emulsion Polymers.* pp. 93-97. New York: John Wiley & Sons, 1997.

14. Dimonie,V.L.; Daniels, E.S.; Shaffer, O.L.; El-Aasser, M.S. Control of Particle Morphology. In P.A. Lovell, and M.S. El-Aasser (eds.), *Emulsion Polymerization and Emulsion Polymers.* pp. 309-316. New York: John Wiley & Sons, 1997.

15. Elmer William B. eds. *The Optical Design of Reflectors.* 2nd ed., New York: Wiley & Sons, 1980.

16. Balakrishnan, T.; Ford Warren, T. Particle Size Control in Suspension Copolymerization of Styrene, Chlorometylstyrene, and Divinylbenzene. *J. Appl. Polym. Sci.*, 27 (1982): 133-138.

17. Okay, O.; Soner, E.; Gungor, A.; Balkas, T.I.; Phase Separation in the Synthesis of Styrene-Divinylbenzene Copolymers with Di-2-ethylhexyl phthalate as Diluent. *J. Appl. Polym. Sci.*, 30 (1985): 2065-2074.

18. Someya, K.; Yamazaki, A.; Hoshino, F.; Yanagihara, T. Multi-Shell Emulsion Particle. *U.S. Pat. 5 500 286,* 1996.

19. Pavlince, J.; Liskova, A.; Lazar, M. Influence of Shear Stress Treatment on Stress-Strain Properties of Methyl methacrylate-Crosslinked Butyl acrylate Core-Shell Polymers. *J. Appl. Polym. Sci.*, 71 (1999): 493-501.

20. Yabuta, M.; Nakao, Y.; Tominaga, A.; High Solids Coatings (Microspheres from Nonaqueous Polymer Dispersions). In Joseph C. Salamone. (eds.), *Polymeric Materials Encyclopedia*, Vol. 5, p. 3017, New York: CRC, 1996.

21. Canche-Escamilla, G.; Mendizabal, E.; Hernandez-Patino, M.J.; Arce-Romero, S.M.; Gonzalez-Romero, V.M. Effect of Morphology on Mechanical and Rheoloigical Properties of Butyl Acrylate-Methyl Methacrylate Multiphase Polymers. *J. Appl. Polym. Sci.*, 56 (1995): 793-802.

22. Olayo, R.; Garcia, E.; Garcia-Corichi, B.; Sanchez-Vazquez, L.; Alvarez, J. Poly (vinyl alcohol) as a Stabilizer in the Suspension Polymerization of Styrene: The Effect of the Molecular Weight. *J. Appl. Polym. Sci.*, 67 (1998): 71-77.

23. Okubo, M.; Izumi, J.; Hosotani, T.; Yamashita, T. Production of Micron-Sized Monodispersed Core/Shell Poly(methyl methacrylate)/Polystyrene Particles by Seeded Dispersion Polymerization. *Colloid Polym Sci.* 8 (1999): 275.

24. Kirsch, S.; Doerk, A.; Bartsch, E.; Sillescu, H. Synthesis of Characterization of Highly Crosslinked, Monodisperse Core-Shell and Inverted Core-Shell Colloidal Particles. Polystyrene/Poly(*tert*-butyl acrylate) Core-Shell and Inverse Core-Shell Particles. *Macromolecules.*, 32 (1999): 4508-4518.

25. Omi, S.; Fujiwara, K.; Nagai, M.; Ma, G.H.; Nakano, A. Study of Particle Growth by Seed Emulsion Polymerization with Counter-Charged Monomer and Initiator System. *Colloids Surface A:Physicochem Eng Aspects*. 153 (1999): 165-172.

26. Jonsson, J-H.; Hassander, H.; Tornell, B. Polymerization Conditions and the Development of a Core-Shell Morphology in PMMA/PS Latex Particles. 1. Influence of Initiator Properties and Mode of Monomer Addition. *Macromolecules.*, 27 (1994): 1932-1937.

27. Chen, Y-C.; Dimonie, V.; El-Aasser, M. S. Interfacial Phenomena Controlling Particle Morphology of Composite Latexes. *J. Appl. Polym. Sci.,* 42 (1991): 1049-1063.

28. Lee, D.I.; Ishikawa, T. The Formation of Inverted Core-Shell Latexes. *J. Polym. Sci. Polym. Chem. Ed.,* 21 (1983): 147-154.

29. Cho, I.; Lee, K-W. Morphology of Latex Particles Formed by Poly(Methyl Methacrylate)-Seeded Emulsion Polymerization of Styrene. *J. Appl. Polym. Sci.,* 30 (1985): 1903-1926.

30. Ma, Q.; Gu, L.; Ma, S.; Ma, G.-H. Study on Synthesis and Morphology Control of Poly(4-vinylpyridine-co-butyl acrylate)/Poly(styrene-co-butyl acrylate) Composite Microspheres. *J. Appl. Polym. Sci.,* 83 (2002): 1190-1203.

31. Okubo, M.; Lu, Y. Preparation of a Heterogeneous Polymer Film from the Blend Emulsion by the Stepwise Heterocoagulation Method. *Colloids and Surfaces A: Physicochem. Eng. Aspects.*, 153 (1999): 609-615.

32. Kemmere, M.F.; Meuldijk, J.; Drinkenburg, A.H., German, A.L. Aspects of Coagulation During Emulsion Polymerization of Styrene and Vinyl Acetate. *J. Appl. Polym. Sci.,* 69 (1998): 2409-2421.

33. Shiozaki, M.; Tokuno, T. Triboelectric Charge Control of Polymer Microspheres by Surface Modification Using Heterocoagulation. *Polym. Int.,* 30 (1993): 217-220.

34. Okubo, M.; Katsuta, Y.; Matsumoto, T. Studies on Suspension and Emulsion. LI. Peculiar Morphology of Composite Polymer Particles Produced by Seeded Emulsion Polymerization. *J. Polym. Sci.: Polym. Let. Ed.,* 20 (1982): 45-51.

35. Muroi, S.; Hashimoto, H.; Hosoi, K. Morphology of Core-Shell Latex Particles. *J. Polym. Sci.: Polym. Chem. Ed.*, 22 (1984): 1365-1372.

36. Kada, T.; Obara, A.; Watanabe, T.; Miyata, S. Fabrication of Refractive Index Distributions in Polymer Using a Photochemical Reaction. *J. Appl. Phys.,* 87 (2000): 638-640.

37. Ulrich, R.; Torge, R. Measurement of Thin Film Parameters with a Prism Coupler. *App. Opt.*, 12 (1973): 2901-2908.

38. Ma, G-H.; Nagai, M.; Omi, S. Study on Preparation and Morphology of Uniform Artificial Polystyrene-Poly(methyl methacrylate) Composite Microspheres by Employing the SPG (Shirasu Porous Glass) Membrane Emulsification Technique. *J. Coll. Int. Sci.* 214 (1999): 264.

39. Takahashi, K.; Miyamori, S.; Uyama, H.; Kobayashi, S. Preparation of Micron-Size Monodisperse Poly(2-hydroxyethyl methacrylate) Particles by Dispersion Polymerization. *J. Polym. Sci. A: Polym. Chem.* 34 (1996): 175.

40. Tawonsree, S.; Omi, S.; Kiatkamjornwong, S. Control of Various Morphological Changes of Poly(meth)acrylate Microspheres and Their Swelling Degrees by SPG Emulsification. *J. Polym. Sci. A: Polym. Chem.* 38 (2000): 4038-4056.

41. Ni, H.-M.; Ma, G.-H.; Nagai, M.; Omi, S. Effects of Ethyl Acetate on the Soap-free Emulsion Polymerization of 4-Vinyl pyridine and Styrene. *J. Appl. Polym. Sci.* 80 (2001): 1988-2001.

42. Samuel, H. Y. *Solubility and Solubilization in Aqueous Media*, 1st ed.; Oxford University Press: New York, 1999; pp. 251-252.

43. Ni, H.-M.; Ma, G.-H.; Nagai, M.; Omi, S. Effect of Ethyl acetate on the Soap-free Emulsion Polymerization of 4-vinylpyridene and Styrene. I. Aspects of the Mechanism. *J. Appl. Polym. Sci.* 82(2001): 2679-2691.

44. El-Aasser, M.S.; Sudol, E.D. Features of Emulsion Polymerization. In P.A. Lovell; and M.S. El-Aasser (eds.) *Emulsion Polymerization and Emulsion Polymers*. pp. 42-44. New York : John Wiley and Sons, 1997.

45. Capek, I. On the Role of Oil-Soluble Initiators in the Radical Polymerization of Micellar Systems. *Advances in Colloid and Interface Science* 2001, 91, 295-334.

46. Nuisin, R.; Ma, G-H.; Omi, S.; Kiatkamjornwong, S. Dependence of Morphological Changes of Polymer Particles on Hydrophobic/Hydrophilic Additives. *J. Appl. Polym. Sci.* 77 (2000): 1013-1028.

47. Ni, H.-M.; Ma, G.-H.; Nagai, M.; Omi, S. Novel Method of Preparation of a Charged Mosaic Membrane by Using Dipole-like Microspheres. II. Preparation of Dumbbell/Egg-like Microspheres. *J. Appl. Polym. Sci.* 80 (2001): 2002-2017.

VITA

Miss Ratsamee Sangsirimongkolying was born in October 28, 1971 in Chonburi, Thailand. She received her Bechelor's degree of Chemistry from the Faculty of Science, Burapha University in 1993 and Master's degree of Chemical Technology from the Faculty of Science, Graduate School, Chulalongkorn University in 1996. She has pursued Doctor Degree of Chemical Technology, Graduate School, Chulalongkorn University since 1998 under the Royal Golden Jubilee Program of the Thailand Research Fund and finished her study in April 2002.